



## **School of Chemistry**

Non-contact polishing of diamond surfaces using dressed photon-phonon etching

Andrew Corbett

This thesis is submitted in partial fulfilment of the requirements for the Honours degree of  
MSci at the University of Bristol

Dr Neil Fox

Professor Paul May

Physical and Theoretical Chemistry



# Declaration

I declare that all contents of this dissertation are my own original work, except where stated and referenced. All experimental work mentioned in this report is my own and no part of this report has been submitted for any other degree. All views expressed in this report are those of the author and in no way represent the views of the University of Bristol. This dissertation has not been presented to any other University in the UK or overseas.

Signature.....

Date.....

# Abstract

A number of CVD diamond surfaces were grown and subjected to dressed photon-phonon etching in order to recreate results achieved by Yatsui *et al.*<sup>1</sup> who realised a superflat single crystalline diamond surface, and an investigation into repeatability of the results on a multicrystalline diamond surface was carried out. The dressed photon-phonon etching was applied to the surface through the use of 254 nm light emitted through UVO treatment. Atomic force microscopy and scanning electron microscopy were used to evaluate the topography of the diamond surface and determine whether the UVO treatment had an observable and quantifiable effect on the roughness of the diamond surface.

The data obtained suggested that dressed photon-phonon etching occurred on the multicrystalline diamond surface but not on a scale or timeframe comparable to that achieved Yatsui *et al.* on a single crystalline diamond surface.

# Contents

Chapter 1. Introduction.....	7
1.1. Diamond .....	7
1.1.1. Uses in modern industry .....	7
1.1.2. Growth of diamonds.....	8
1.1.3. Superflat surfaces.....	11
1.1.4. Diamond polishing modes.....	11
1.1.5. Roughness Analysis .....	12
1.2. Dressed Photon-Phonon Etching.....	13
1.2.1. Radical Theory.....	13
1.2.2. Dressed Photons and Dressed Photon-Phonon interactions.....	14
Chapter 2. Experimental Procedure .....	16
2.1. Chemical Vapour Deposition.....	16
2.2. UVO Cleaner .....	16
2.3. Microscopy .....	18
2.3.1. Scanning Electron Microscopy.....	18
2.3.2. Atomic Force Microscopy.....	19
Chapter 3. Results .....	20
3.1. Pre-treatment images .....	20
3.2. Post-treatment images.....	24
3.3. Surface Roughness Analysis .....	34
Chapter 4. Discussion .....	37
4.1. Overview.....	37
4.2. Qualitative Analysis.....	37
4.3. Quantitative Analysis .....	44
Chapter 5. Conclusion.....	47
5.1. Overview.....	47

# Acknowledgements

I would like to take the time to thank everyone who has given me support and advice throughout the duration of this project. A large amount of thanks goes to everyone in the University of Bristol CVD Diamond Group for everything that they have all done to assist me in my project.

I would also like to thank Mr Jonathon Jones and Mr Robert Harniman of the University of Bristol Electron Microscopy Unit for spending a lot of their time helping me to obtain the perfect images of my surfaces.

A big thank you goes to Miss Sarah Halliwell, who gave a lot of her time to answer many questions I had throughout the year.

And finally, a lot of thanks goes to my primary supervisor, Dr Neil Fox, for helping me with any dead ends I came to in my project, and encouragement throughout the year.

# CHAPTER 1. INTRODUCTION

## 1.1. Diamond

Diamond has long been known for possessing highly sought after physical properties, such as extreme hardness, thermal conductivity<sup>2</sup> and many more, spread over a huge range of applications. However, due to the extreme scarcity of diamond as a natural resource, diamond was unable to be widely used in scientific applications for many years and was mainly used purely for decorative purposes as a precious mineral. Over the last century, research into the synthetic growth of diamond has progressed dramatically, leading to a great increase in the availability of diamond surfaces, and thus also in the use of diamonds in a wide array of modern industry. This has led to research into the implementation of diamonds surfaces as substrates in a wide range of industrial uses<sup>3</sup>.

However, the use of synthetically grown diamonds in industry is somewhat limited by the surface roughness and non-uniform characteristics of the microcrystalline surface<sup>4</sup>. A number of contact polishing processes are available but due to the extreme properties of diamond, these are impractical and this project extends research into non-contact polishing processes, in particular dressed photon-phonon etching, and determining whether non-contact polishing methods are suitable for creating uniform, flat diamond surfaces.

### 1.1.1. Uses in modern industry

Although large, natural diamonds are a scarce resource, synthetic diamonds are a material prevalent in modern industry. The many extreme properties of diamond render it an ideal material to be used in a large number of different applications, mainly due to high resistance to external forces. For many years the toughness of diamond has been utilised in construction industries as dust, grit, and small fragments in order to act as an enhanced abrasive or cutting tool<sup>5</sup>, but since the advent of synthetic diamond as a widespread resource, synthetic diamond has been used in many different industrial applications. Diamond films have been deposited on titanium alloys Ti-6Al-4V and Ti-6Al-7Nb in order for use in the aerospace and biomedical industries<sup>6</sup>, and the resistance of diamond to extreme

temperatures and a high dielectric constant leads to diamonds being a sought after material for use in high temperature capacitors<sup>7</sup>. Diamond films can also be used as radiation detectors<sup>8</sup>; as heat sinks<sup>9</sup> and high power laser windows<sup>10</sup>. As shown, the properties of diamond can be utilised in many diverse applications, and this is only made possible by the advancement of synthetic diamond growth technology, allowing diamond to become a common and easy to obtain material.

## 1.1.2. Growth of diamonds

A number of different techniques for the growth of synthetic diamonds in the laboratory have been used since the discovery of synthetic diamonds. Historically, high-temperature, high-pressure (HTHP) systems have been used to synthesise diamond by imitating the conditions which enable the growth of natural diamond. Bundy *et al.* (1955)<sup>11</sup> first describe a reproducible technique used to synthesise diamond using HTHP apparatus, and gave proof that diamond was yielded, due to diamond being the thermodynamically stable product under the apparatus conditions. However, it has since been discovered that the diamond present in this ground-breaking experiment was a fragment of a natural type Ia diamond<sup>12</sup> and not the so-claimed synthetic diamond, although the technique used has held up to scrutiny and been used to successfully synthesise diamonds for many decades<sup>13</sup>.

Although this was a system successfully used for many decades, HTHP apparatus has many shortcomings. For example, the extreme conditions needed for this system leads to high equipment and maintenance costs, and if similar results could be obtained without the need for such extreme conditions there would be an obvious cost benefit. Eversole (1958)<sup>14</sup>, Deryagin *et al.* (1968)<sup>15</sup> and Angus *et al.* (1968)<sup>16</sup> conducted investigations into the possibility of building diamond from an initial template in the gas phase, as the use of the gas phase could take place under more mild conditions at a lot lower pressure than previous systems and thus be much more economically viable. This is achieved through Chemical Vapour Deposition (CVD) techniques, a process through which an epitaxial layer of diamond is built-up on a non-diamond surface in order to create a thin film diamond surface<sup>17</sup>. This system is very useful because the non-diamond surface can be used as a template and thus the shape of the synthetic diamond created can be prespecified.

Whereas in HTHP systems, diamond is the thermodynamically stable phase of the carbon, in a CVD system, diamond is a metastable phase<sup>18</sup>; meaning that a number of conditions must be observed in order to ensure only diamond is deposited on the surface, not graphite,

and that diamond growth exceeds graphitisation of the diamond surface. A technique that greatly helps this is the presence of an excess of hydrogen in the system<sup>19</sup>. This is because addition of hydrogen can prevent formation of a number of aromatic species that are responsible for the deposition of graphitisation forming in the gas phase<sup>20</sup>.

There are a number of processes through which CVD diamond can be synthesised but these mainly differ on apparatus specifics, the underlying theory is common ground between the methods. CVD is caused by gas phase chemistry close to the target surface, and thus a process gas containing precursor molecules must be present in the system which can be something as simple as a hydrocarbon such as methane in an excess of hydrogen<sup>21</sup>. The gas phase containing these precursor molecules is then activated through decomposition in order to create atomic hydrogen from the H<sub>2</sub> excess<sup>22</sup>, which then ensures preferential growth of diamond as opposed to other carbon forms. Figure 1 shows the process through which the diamond surface is built up, through the exploitation of the highly reactive nature of the radical species which were created through the activation of the precursor molecules. The radical species can attack the diamond surface, creating radical species on the surface, which can then be stabilised by further radical attack resulting in a diamond surface build-up. The build-up of diamond surfaces is an amorphous process<sup>23</sup>, leading to non-uniform microcrystal sizes with surface roughness greatly varying across the multicrystalline surface and thus techniques must be implemented in order to create a flat and uniform surface.

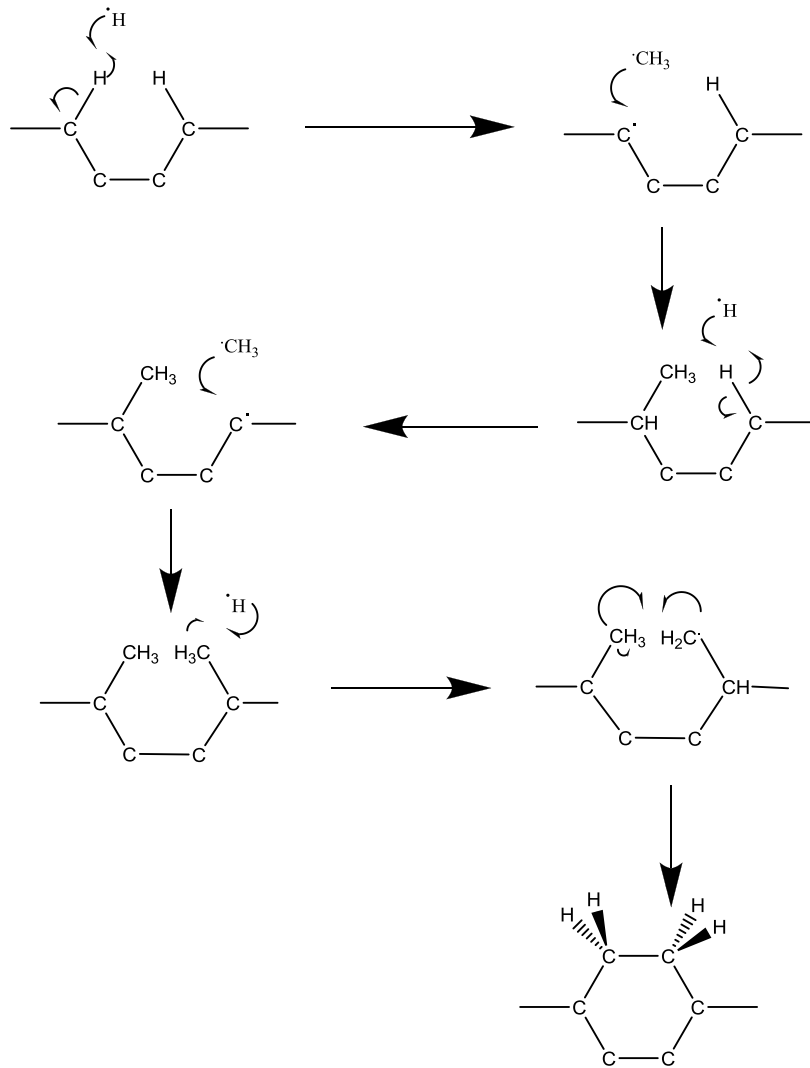


**Figure 1:** A schematic showing the growth of diamond occurring at the surface by addition of  $\text{CH}_3$  and  $\text{H}$ .

Adapted from P.W. May, "Diamond Thin Films: A 21st Century Material" *Phil. Trans. R. Soc. Lond. A*, **358**, 473 – 495, (2000)

There are three main systems for the synthesis of CVD diamond: "hot filament chemical vapour deposition (HFCVD); high frequency microwave plasma-assisted chemical vapour deposition (MW-PACVD); and DC plasma discharge"<sup>24</sup>. These differ in the technique used to activate the gas phase in the system and differences between the various systems are shown in Figure 2. HFCVD uses a hot metal filament a small distance from the substrate surface to thermally decompose the gas phase, leading to the creation of atomic hydrogen and hydrocarbon radical species, which can then lead to the build-up of a diamond surface. MW-PACVD systems utilise a high frequency microwave in order to enhance the reactivity gas phase by forming hydrocarbon radical species and atomic hydrogen which leads to the

build-up of a diamond surface<sup>25</sup>. DC plasma discharge CVD systems utilise a hot filament with dc discharge plasma to lower the level of heating applied to the gas phase<sup>26</sup> which then leads to the formation of hydrocarbon radical species and atomic hydrogen, which generates diamond surface build-up.

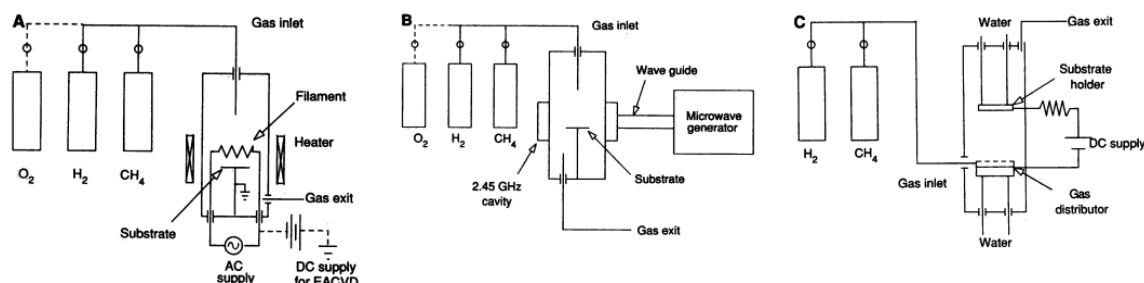


**Figure 2:** Schematic showing the systems used in HFCVD (A), MW-PACVD (B), and DC plasma discharge (C).

From Angus, J. C., Hayman, C. C., *Science*, **241**, 4868, 913-921 (1988)

### 1.1.3. Superflat surfaces

The growth of CVD diamond surfaces will lead to the production of a diamond surface with high levels of surface roughness, which can place limitations on the applications of the diamond surface in industry. Ideally, the process would create a superflat, uniform surface with diamonds of identical size and orientation, and although this is impossible in practice, there are a number of polishing modes which can be applied in order to optimise the characteristics of the diamond surface.

Superflat diamond surfaces substrates are needed for potential high performance industrial and commercial uses in a wide range of fields. For example, power devices using boron doped diamond surface substrates show potential high performance using superflat surfaces<sup>27</sup> and light emitting diodes can produce extremely high performance when superflat diamond substrates are used<sup>28</sup>.

### 1.1.4. Diamond polishing modes

In order to obtain a superflat diamond surface, a polishing system must be laid in place to change the morphology of the non-uniform diamond surface. A popular polishing mode is

chemical-mechanical polishing (CMP) which uses chemical and mechanical processes to erode diamond surfaces in order to decrease the surface roughness and create a more uniform substrate surface. There are a number of different approaches to CMP for a diamond surface. For example, use of an abrasive slurry to wear through the diamond surface with friction<sup>4</sup> that can break micro-chips of diamond off the surface, leading to lower surface roughness. Chemical assistance can also be used, with the presence of oxidising agents increasing the removal rate of micro-chips from the surface<sup>29</sup>.

However, contact polishing methods of diamond surfaces are somewhat impractical due to high resistance of diamond to erosion, and thus a high input of energy is needed to overcome the extreme properties of diamond. Non-contact polishing methods of reducing the surface roughness of diamond can be used as an alternative to contact polishing methods, and these processes can be much more energy efficient, and do not need any chemical assistance, and thus can be more cost-effective, whilst also producing more uniform and superflat surfaces, such as the dressed photon-phonon etching process, as will be addressed in this project.

### **1.1.5. Roughness Analysis**

The roughness of a diamond surface can be analysed in a number of different ways. The most common method for calculating surface roughness is the average roughness ( $R_a$ ), which is simply the arithmetic average of the displacement from the plane of best fit of the absolute values of the surface height, as shown in Equation 1. This is used historically, due to many older instruments being unable to perform other surface roughness calculations. However, due to this being an oversimplified method, there are a number of shortcomings, such as there being no differentiation between whether an imperfection in the surface is a valley or peak, so inaccuracies may be gained in results because over a measured area, these may compensate for each other and give a lower roughness value than what is correct.

Root Mean Square Roughness ( $R_{RMS}$ ) uses a square method of calculating the surface roughness of an area, which minimises the aforementioned inaccuracies. This means that troughs and peaks can be distinguished due to the distance from the plane of best fit being squared and thus negative and positive values can be combined instead of compensating for each other. Thus  $R_{RMS}$  values should be larger than  $R_a$  values.

There are a number of other processes that can characterise surface roughness, such as skewness, and measurements involving first and second derivatives of the surface profile which can be utilised to investigate the curvature of the surface<sup>30</sup>, but  $R_a$  and  $R_{RMS}$  are the processes used for the purposes of this project seeing as these can be rapidly calculated from the raw data and will give enough information to characterise the diamond surfaces.

$$R_a = \frac{y_1+y_2+y_3+y_4+\dots+y_n}{n} \quad [1]^{31}$$

$$R_{RMS} = \left( \frac{y_1^2+y_2^2+y_3^2+y_4^2+\dots+y_n^2}{n} \right)^{\frac{1}{2}} \quad [2]^{31}$$

## 1.2. Dressed Photon-Phonon Etching

Dressed photon-phonon etching is the main process behind non-contact polishing of diamond surfaces, utilising dressed photon-phonon interactions to ensure that bond-breaking only occurs at the desired parts of the surface. In the case of non-contact polishing, the desired areas of the surface for bond-breaking to occur are at local peaks, in order to create a flatter surface. Dressed photon-phonon etching relies on a number of processes in order to break bonds at the desired points of the diamond surface which in turn can lead to realisation of a superflat surface. Yatsui *et al.* have developed a process for non-contact polishing using dressed photon-phonon interactions on a single crystalline diamond surface<sup>1</sup> and investigation into whether similar processes are feasible for multicrystalline diamond surfaces is undertaken in this project. A great advantage of dressed photon-phonon etching for use as a non-contact polishing mode is that all that is needed is the presence of oxygen, which can be obtained from the environment, and photons of the correct energy, which can be provided by relatively cheap, low energy apparatus and no mechanical work is needed, unlike many contact polishing modes.

### 1.2.1. Radical Theory

Dressed photon-phonon etching leads to the creation of highly reactive radical species in order to generate flat diamond surfaces. This is due to radical theory which shows how

radical species can be utilised to break chemical bonds. The highly reactive character of radical species was demonstrated in Figure 1 which showed that atomic hydrogen and  $\text{CH}_3$  radical species were used to attack the surface of a diamond in order for CVD build-up of the diamond surface to occur and this highly reactive nature can be exploited for non-contact polishing. In the case of Yatsui *et al.* oxygen radical species were formed at the diamond and were able to breakdown the diamond surface through an etching process. Oxygen radical species are able to etch the diamond surface due to the extremely highly oxidative characteristic of atomic oxygen<sup>32</sup> and thus oxidise the diamond surface, forming carbon monoxide by ripping carbon atoms from the diamond lattice, and thus causing breakdown and etching of the diamond surface.

The formation of atomic oxygen at the diamond surface would cause isotropic etching of the substrate surface which would not decrease the surface roughness and would simply decrease the thickness of the substrate. However, the energy of the photons used by Yatsui *et al.* and in this project is not high enough to dissociate atmospheric  $\text{O}_2$  through a standard photochemical reaction, due to the use of photons with energies of 3.81 eV<sup>1</sup> and 4.88 eV respectively, and the dissociation energy of  $\text{O}_2$  is 5.5 eV<sup>33</sup>. Due to dressed photon-phonon interactions, formation of oxygen radicals through a standard photochemical reaction does not occur, and radical species formation occurs preferentially at the peaks of the diamond surface, resulting in defined etching which decreases the surface roughness of the diamond substrate.

## **1.2.2. Dressed Photons and Dressed Photon-Phonon interactions**

Dressed photons are quasi-particles that can be formed through the coupling of a virtual photon to an electron in the optical near-field<sup>34</sup>. A virtual photon is a short-lived species that can be re-absorbed by the electron but can also couple with the electron in a very distinct way, which means that the virtual photon-electron coupling, or dressed photon, now carries the energy of excitation of the electron, thus the dressed photon carries more energy than a free photon. A theoretical description of the dressed photon state can be “described by assuming a multipolar quantum electrodynamic Hamiltonian in a Coulomb gauge and single-particle states in a finite nano-system”<sup>35</sup>.

In the case of Yatsui *et al.* a photon with wavelength 325 nm (3.81 eV) is coupled to an electron to form a dressed photon, and in this project, a photon with wavelength 254 nm (4.88 eV) can become coupled to an electron to form a dressed photon.

As stated, dressed photons have higher energies than free photons of the same wavelength due to the electron coupling, and the energy of the dressed photon can be increased through the coupling of a dressed photon to a phonon to form a dressed photon-phonon quasi-particle<sup>36</sup>. This dressed photon-phonon coupling interaction can occur when the energy of the dressed photon causes a “multi-mode coherent phonon state”<sup>34</sup> with the vibrational modes of a particle surface<sup>37</sup>, which can occur on an imperfect diamond surface due to the peaks on the diamond surface acting as optical near-field nanometric probe tips<sup>38</sup>.

In this way, dressed photon-phonon coupling interactions can occur and form a quasi-particle of higher energy than the free photon due to the coupling interactions. In the case of Yatsui *et al.*, where the free photon is of too low energy to photochemically dissociate the etching gas, the higher energy dressed photon-phonon quasi-particles can preferentially dissociate the etching gas at the diamond surface peaks, due to the quasi-particle energy exceeding the dissociation energy of the etching gas. Thus the dressed photon-phonon quasi-particles forming oxygen radical species which selectively etch the diamond surface peaks leading to the realisation of a superflat diamond surface through dressed photon-phonon etching as a non-contact polishing process<sup>1</sup>.

# CHAPTER 2. EXPERIMENTAL PROCEDURE

## 2.1. Chemical Vapour Deposition

The diamond surface substrates used in the project were grown using an HFCVD system under slightly different conditions in order to determine whether the deposition time would have an effect on the dressed photon-phonon etching of the diamond surface.

Diamond substrate 1 was grown at 20 Torr, using a rhenium filament at a current of 25 A at 1073 K, on p-type silicon substrate with a deposition time of 4 hours. The flow rates were 0.1 standard cubic centimetres per minute (SCCM) B<sub>2</sub>H<sub>6</sub>, 2 SCCM CH<sub>4</sub>, and 200 SCCM H<sub>2</sub>. The thickness of the substrate was 2 μm.

Diamond substrate 2 was grown at 20 Torr, using a rhenium filament at a current of 25 A at 1073 K, on a p-type silicon substrate with a deposition time of 3.5 hours. The flow rates were 0.1 SCCM B<sub>2</sub>H<sub>6</sub>, 2 SCCM CH<sub>4</sub>, and 200 SCCM H<sub>2</sub>. The thickness of the substrates was 1.5 μm.

## 2.2. UVO Cleaner

The exposure to 254nm UV light was carried out using a Jelight UVO Cleaner 42A-220. This model also emits light at 185nm which instantaneously produces atomic oxygen from atmospheric oxygen. In order to reduce the level of 185nm light and atomic oxygen exposure to the diamond surface, the diamond substrate was encased in a glass box with a diamond window. The diamond window was opaque to UV light below a certain wavelength and thus could block out the 185nm light. The glass box minimised the level of atomic oxygen that came in contact with the diamond surface in order to stop undefined destruction of the diamond surface. However, the glass box was not airtight due to the need of O<sub>2</sub> molecules in order for dressed photon-phonon etching to occur, and in a closed system there is only a

finite supply, but the level of atomic oxygen present at the diamond surface was deemed negligible.

Each substrate was subjected to a number of hours of treatment, with examination after set intervals. The UVO cleaner was not used for more than two hours at one time to prevent overheating.

The UVO cleaner has an output peak-peak voltage of 6000 V and output current of 30 mA. The 254 nm light was emitted at an intensity of 28-32 mW/cm<sup>2</sup>.

Substrate 2 was separated into 5 segments in order to examine 5 different levels of treatment simultaneously. Each segment was labelled and treated for two hours longer than the previous segment as shown in Figure 3. The segment separation and segment number labelling were performed using a laser cutter, ensuring the grooves were shallow enough so as not to minimise the possibility of a snap occurring, a FEGSEM image showing the resulting substrate before any treatment occurred is shown in Figure 4. An aluminium sheet was used as a shield to block the 254nm light from the diamond surface in order to ensure dressed photon-phonon etching was only occurring in specific segments.

1	2	3	4	5
2 hrs treatment	4 hrs treatment	6 hrs treatment	8 hrs treatment	10 hrs treatment

**Figure 3:** Schematic showing segments of Substrate 2, number labelling, and number of hours of treatment received

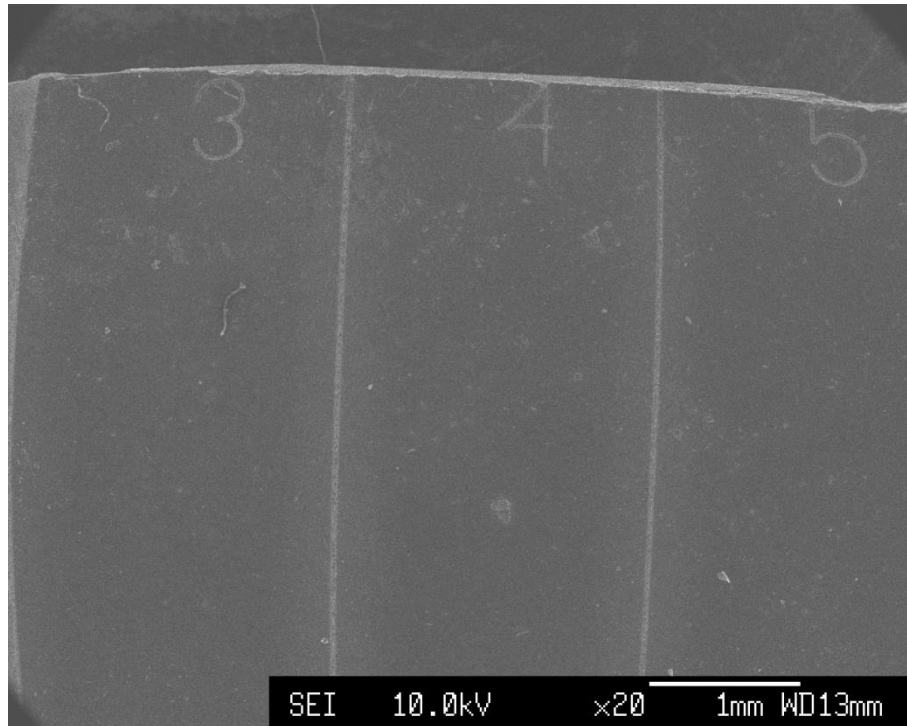


**Figure 4:** FEGSEM image showing the number labelling and segment separation of segments 3, 4 and 5 of the untreated surface of substrate 2

## 2.3. Microscopy

A number of microscopy techniques were used to observe the effect of the dressed photon-phonon etching on the diamond surface and evaluate the topography of the surfaces throughout the process. The main techniques used were Scanning Electron Microscopy (SEM) and Atomic Force Microscopy (AFM). These techniques were utilised both before and after treatment in the UVO Cleaner in order to ascertain the change in characteristic and the topography of the diamond surface.

### 2.3.1. Scanning Electron Microscopy

A Field Emission Gun Scanning Electron Microscope (FEGSEM) was used to conduct the scanning electron microscopy. The images were taken at a working distance of 15 mm at a

current of 12  $\mu\text{A}$  and a voltage of 10 kV. The images taken were over a large range of magnifications, from x20 through to x75 000.

### **2.3.2. Atomic Force Microscopy**

A Nanoscope Atomic Force Microscope (AFM) was used to conduct the atomic force microscopy. A tapping mode was used, so that the surface profile of the substrate may be closely examined after each treatment. Use of the tapping mode ensured that a highly accurate image was obtained due to production of a three-dimensional representation of the diamond surface.

The images recorded have an image size of 512 x 512 pixels, with a scan rate of 0.125 lines  $\text{s}^{-1}$ . The area of the images recorded was 100  $\mu\text{m}^2$ , thus the resolution of the images produced was 0.0381  $\mu\text{m pixel}^{-1}$ .

The AFM data could be used to evaluate the surface roughness of the substrates due to the realisation of a topographical surface profile which gives accurate data of the height of each pixel. Thus each AFM image has a large amount of surface data which can be used to calculate  $R_a$  and  $R_{\text{RMS}}$  for the diamond surfaces.

# CHAPTER 3. RESULTS

## 3.1. Pre-treatment images

The images obtained through the microscopy of the diamond surfaces before any UVO treatment was performed are shown.

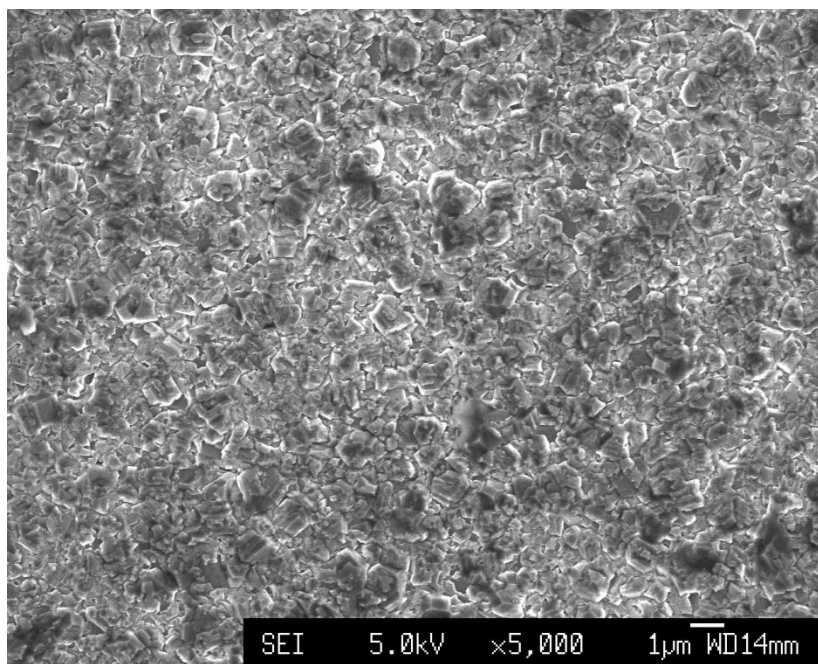


**Figure 5:** FEGSEM image of the surface of substrate 1 taken before any treatment was performed. An overview of the substrate surface at x5 000 magnification

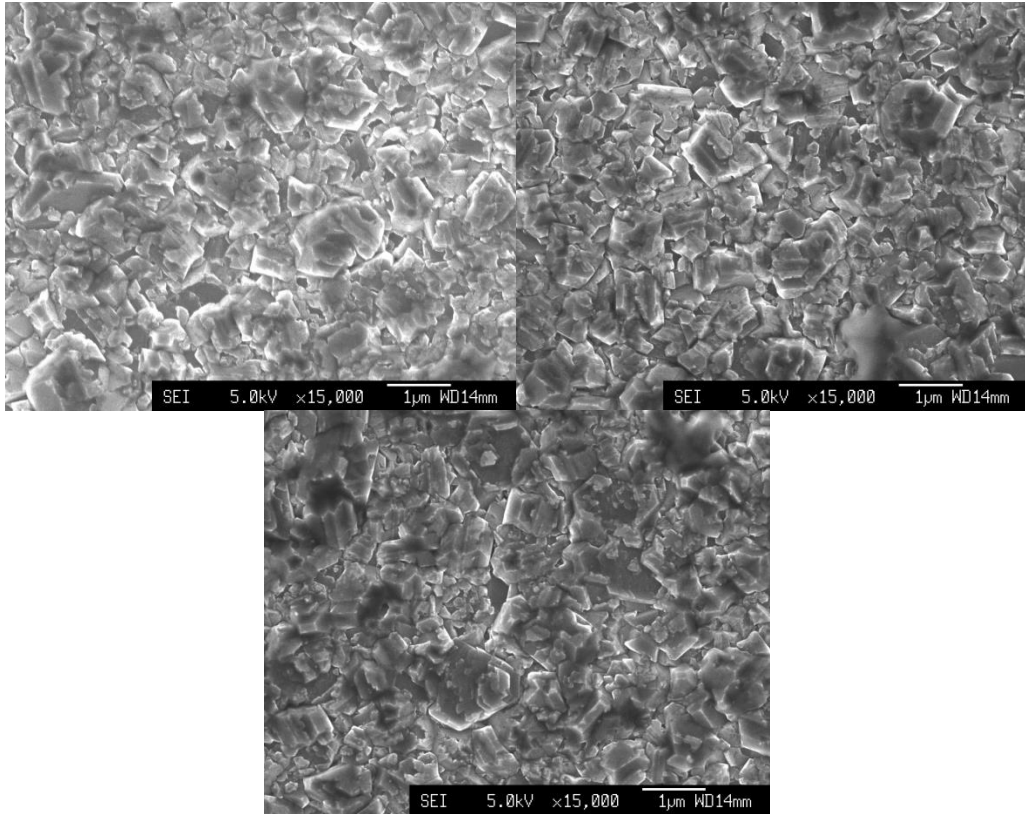


**Figure 6:** FEGSEM images showing the untreated surface of substrate 1 at x15 000 magnification

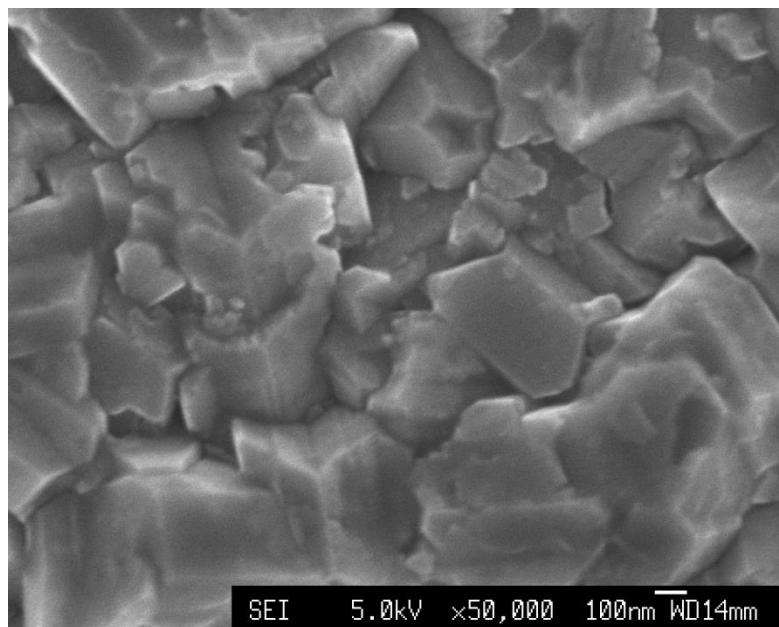


**Figure 7:** FEGSEM image showing the untreated surface of substrate 1 at x50 000 magnification

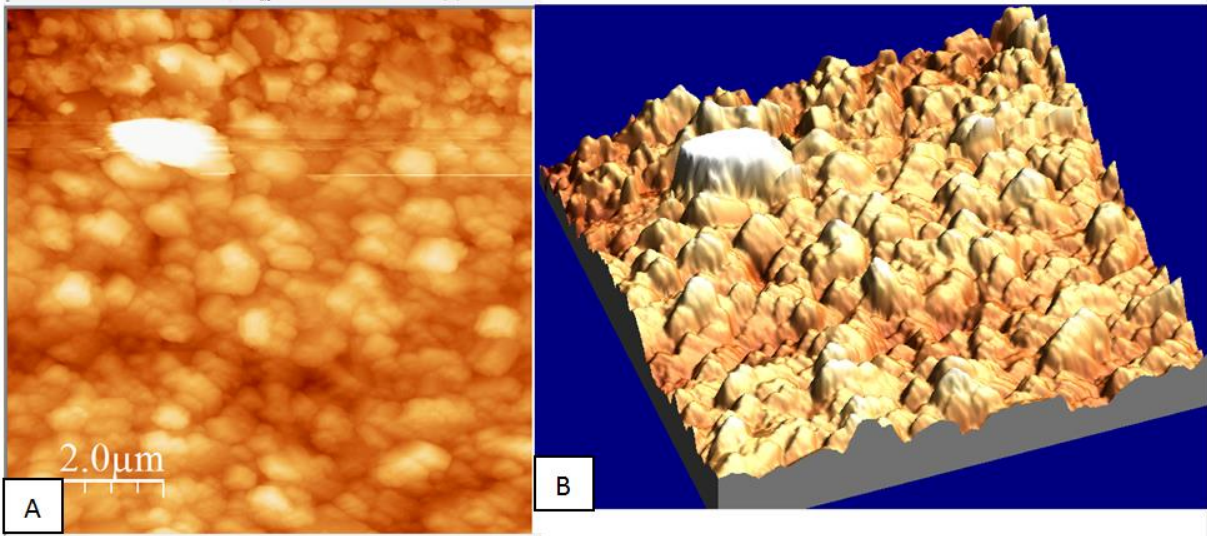


**Figure 8:** Images of the surface of substrate 1 taken before any treatment using the atomic force microscope. A) Shows a 100 μm<sup>2</sup> area of the sample B) Shows the same image as a three dimensional representation

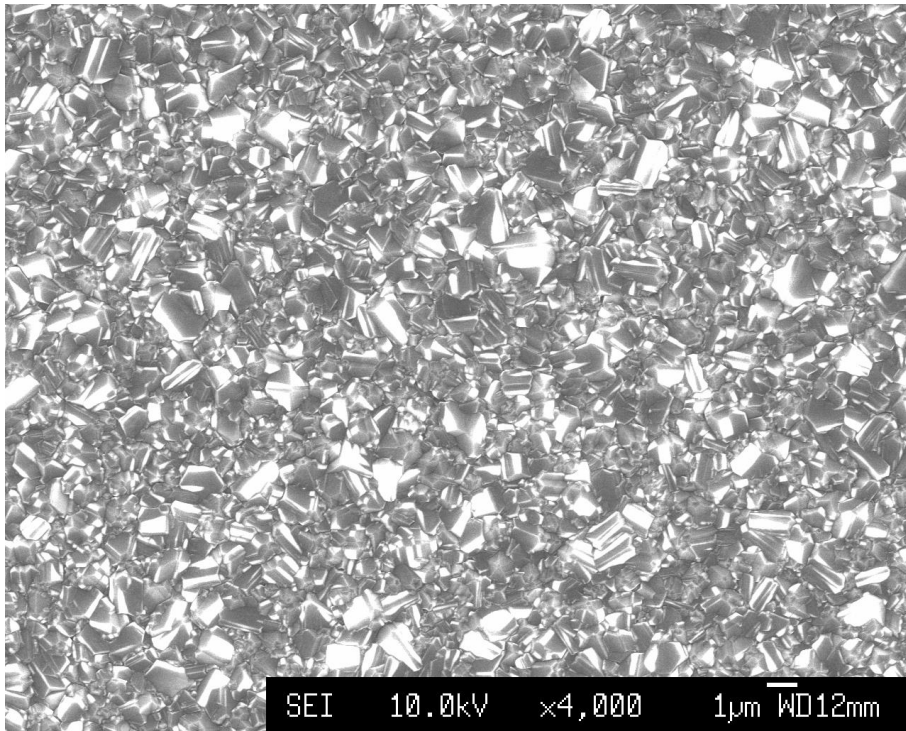


**Figure 9:** FEGSEM image showing an overview of the untreated surface of substrate 2 at x4 000 magnification

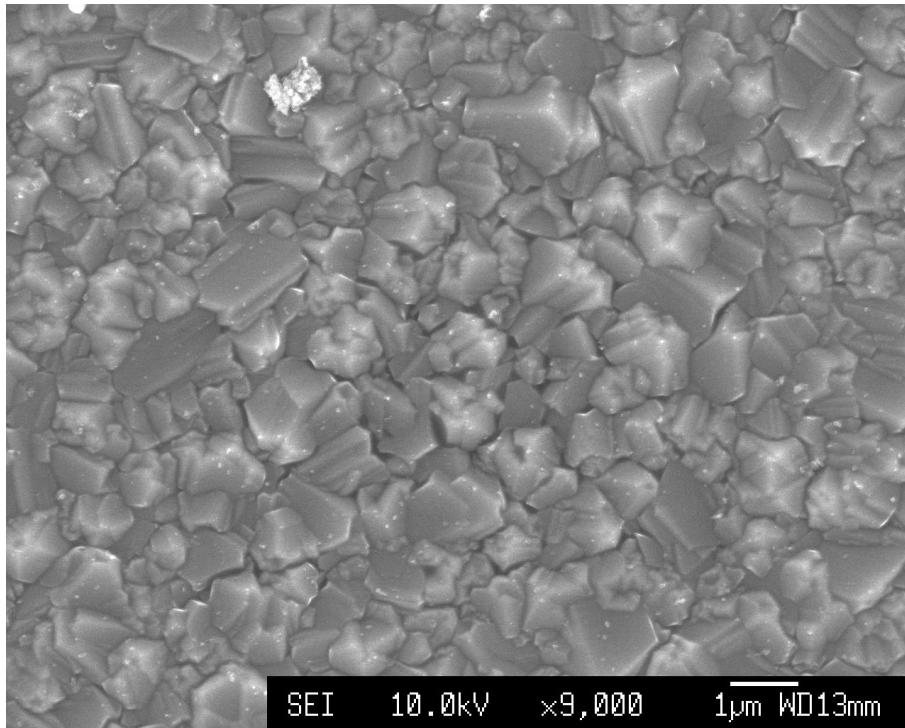


**Figure 10:** FEGSEM image showing an overview of the untreated surface of substrate 2 at x9 000 magnification

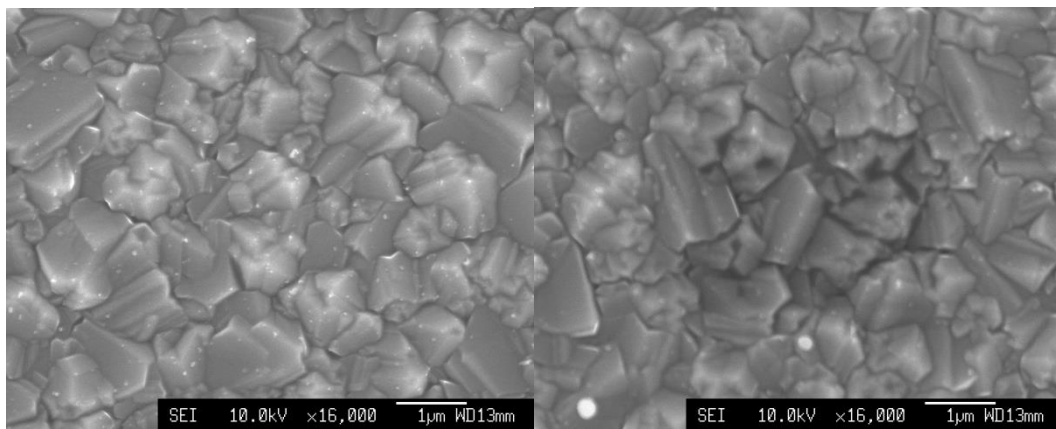


**Figure 11:** A number of FEGSEM images of substrate 2 surface characteristic at x16 000 magnification

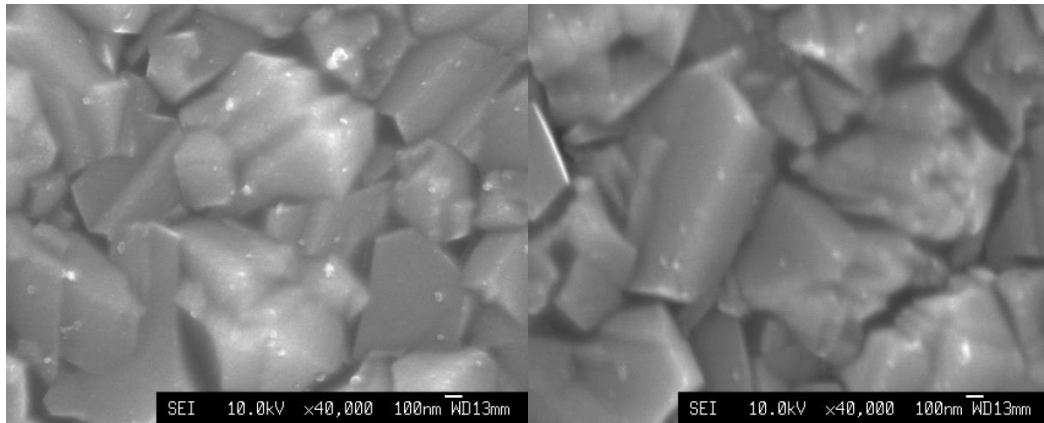


**Figure 12:** A number of FEGSEM images of substrate 2 at x40 000 magnification showing details of the surface characteristic

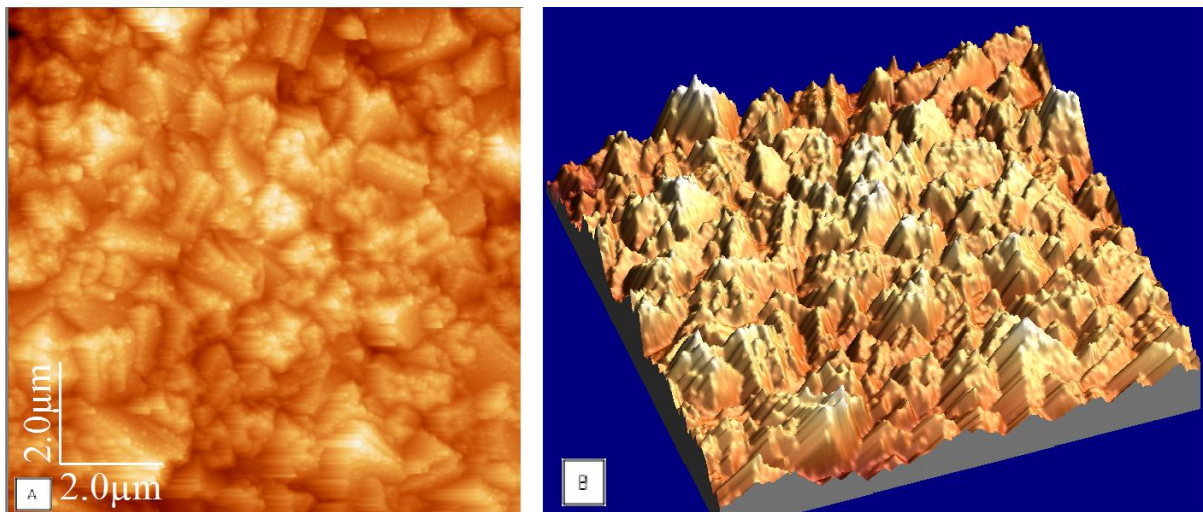


**Figure 13:** AFM images of the surface of substrate 2 taken before any treatment. A) Shows a  $100 \mu\text{m}^2$  area of the sample B) Shows the same image as a three dimensional representation

## 3.2. Post-treatment images

The substrates were imaged after set time intervals, for substrate 1 this occurred after 1, 3, 4 and 6 hours, and for substrate 2 this occurred when the treatments were all finished with segments 1 – 5 having undergone treatment for 2 – 10 hours respectively. Examples of FEGSEM and AFM images of the two substrates are shown in Figures 14 – 30. These can

show the visual effect of the UVO treatment on the surfaces and the AFM images can give topographical data which can be used to analyse the surface roughness.

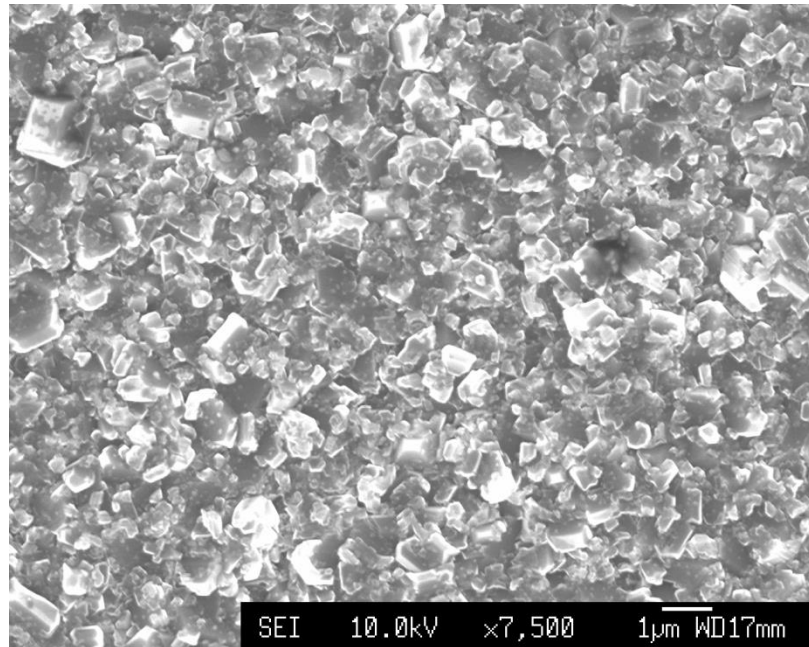


**Figure 14:** FEGSEM image showing overview of substrate 1 after 1 hour UVO treatment at x7 500 magnification

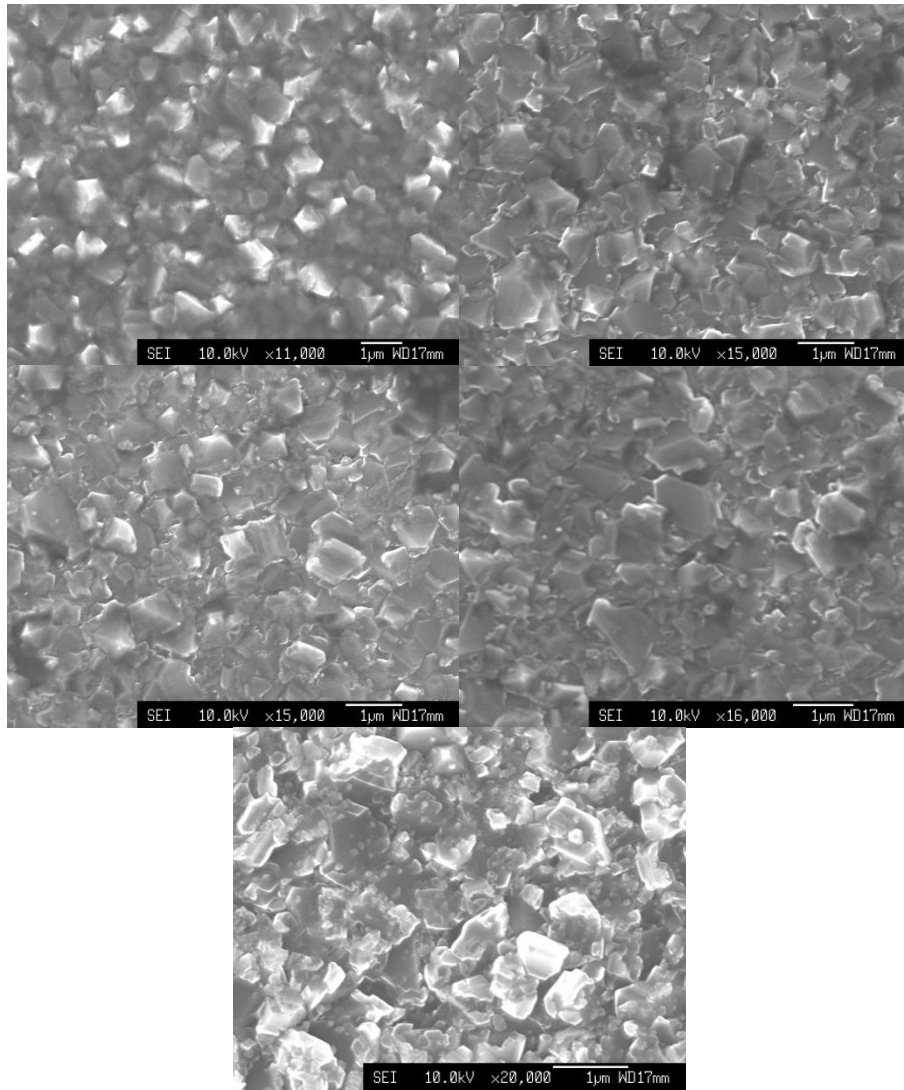


**Figure 15:** FEGSEM images of substrate 1 after 1 hour UVO treatment. Images taken at various magnifications increasing from x11 000 – x20 000

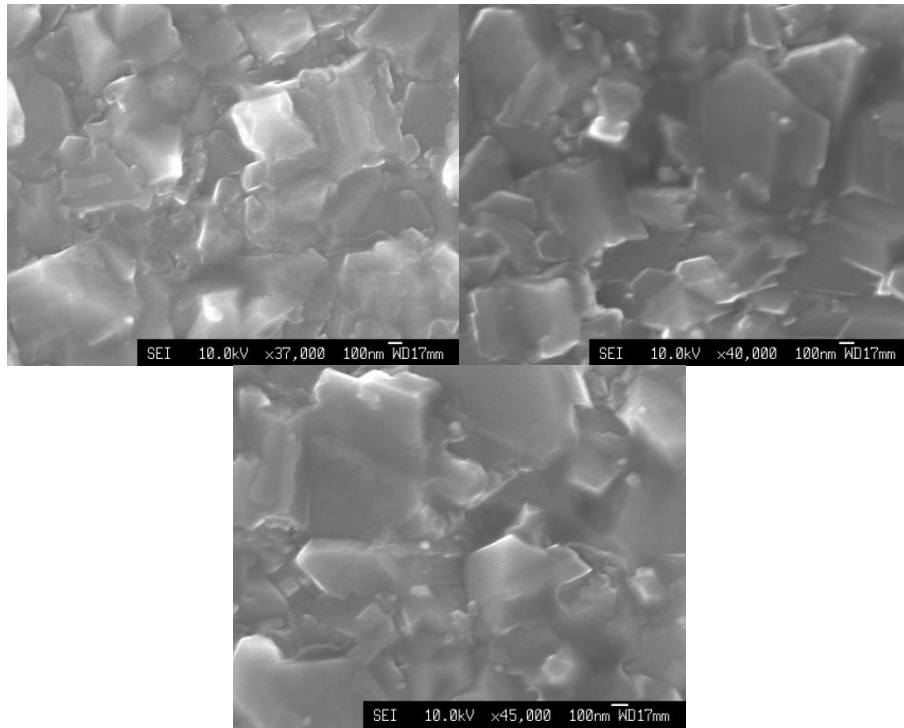


**Figure 16:** FEGSEM images of substrate 1 after 1 hour UVO treatment. Images taken at various magnifications increasing from x37 000 – x45 000

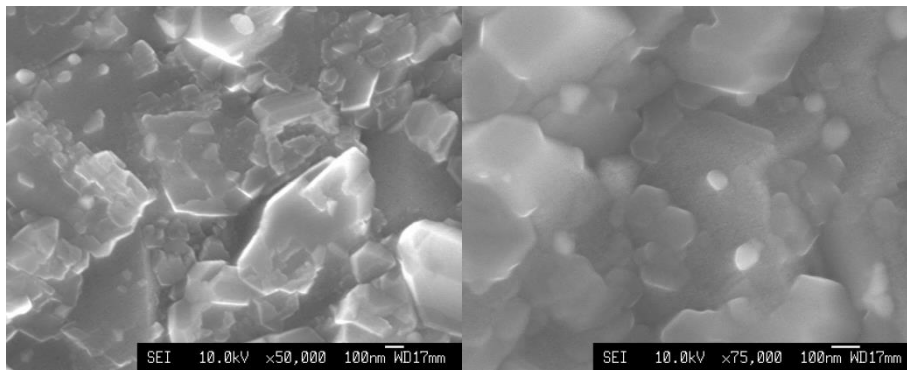


**Figure 17:** High detail FEGSEM images of substrate 1 after 1 hour UVO treatment. Images taken at x50 000 and x75 000 magnification

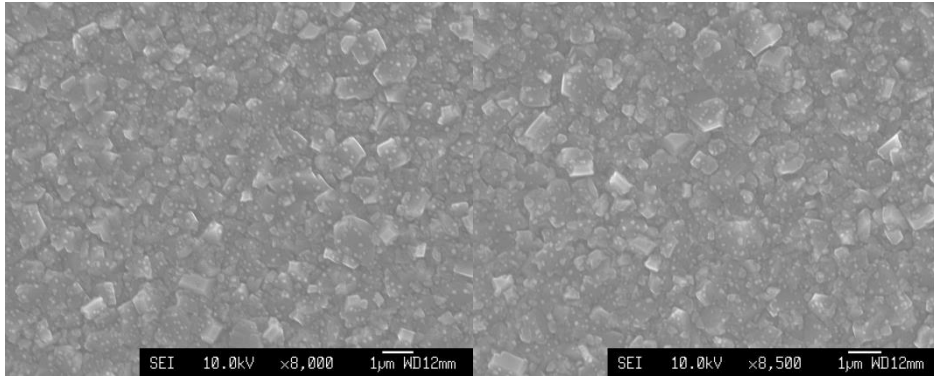


**Figure 18:** FEGSEM images showing overview of substrate 1 after 2 hours UVO treatment. Images taken at x8 000 and x8 500 magnification

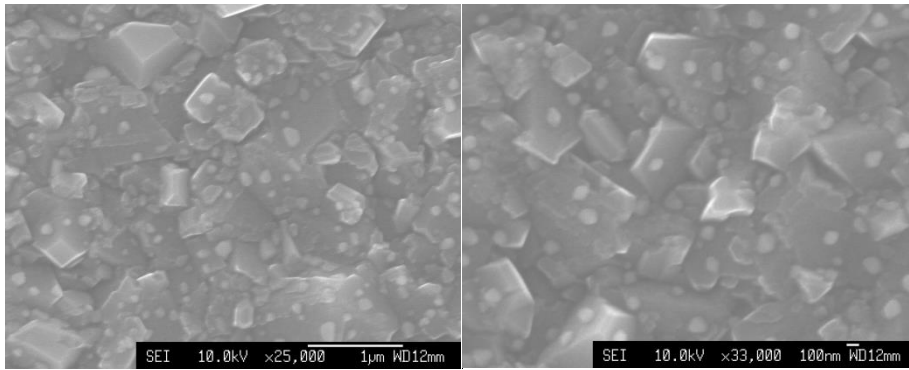


**Figure 19:** FEGSEM images showing substrate 1 after 2 hours UVO treatment. Images taken at x25 000 and x33 000 magnification

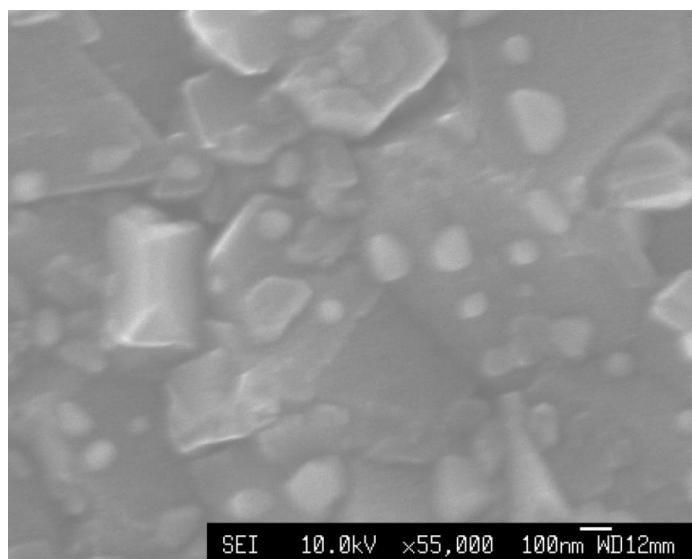


**Figure 20:** High detail FEGSEM images of substrate 1 after 2 hours UVO treatment. Image taken at x55 000 magnification

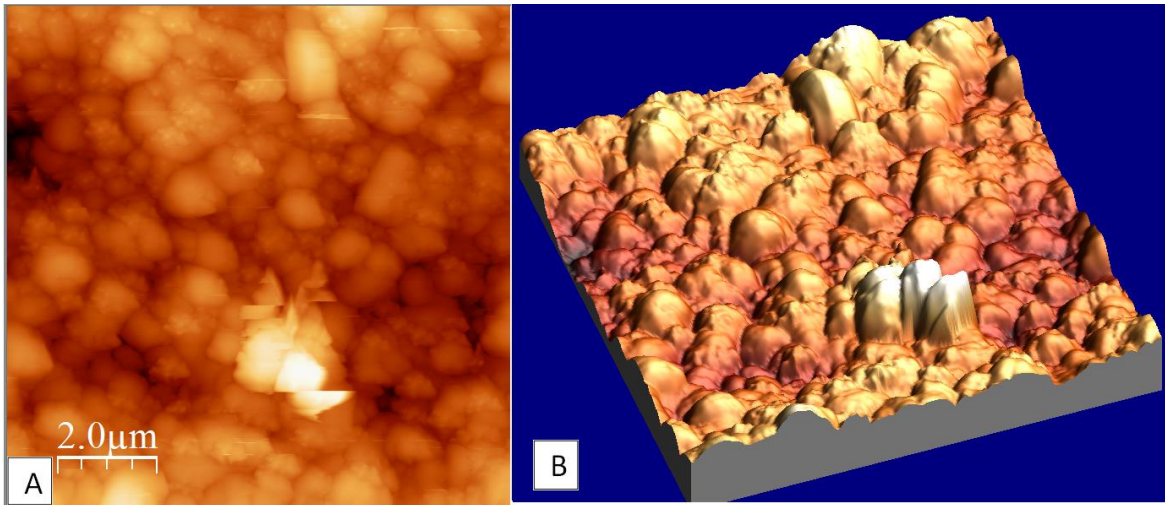


**Figure 21:** AFM images of the surface of substrate 1 taken after 2 hours UVO treatment. A) Shows a  $100\ \mu\text{m}^2$  area of the sample B) Shows the same image as a three dimensional representation

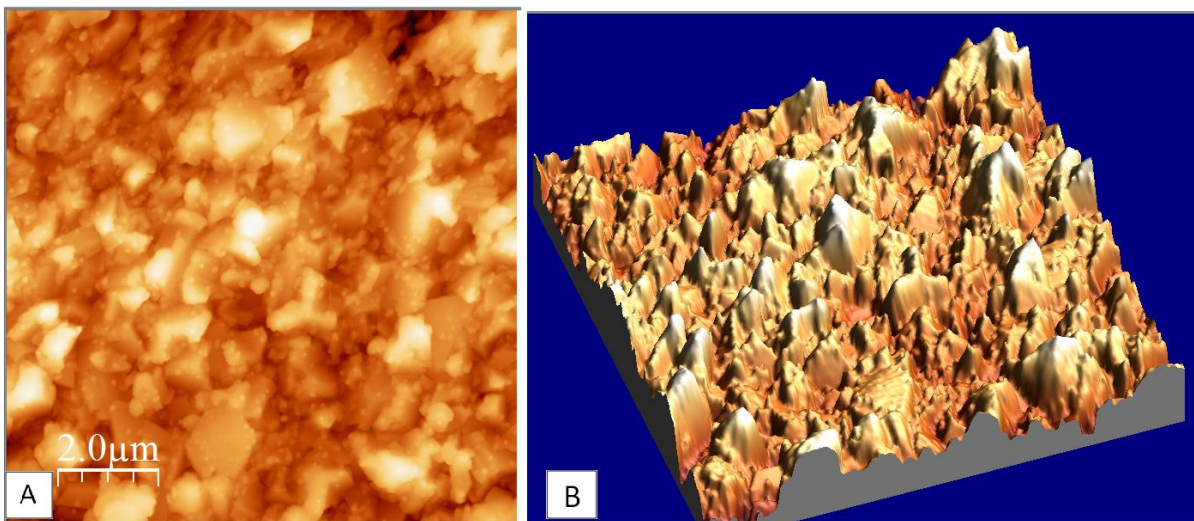


**Figure 22:** AFM images of the surface of substrate 1 taken after 3 hours UVO treatment. A) Shows a  $100\ \mu\text{m}^2$  area of the sample B) Shows the same image as a three dimensional representation

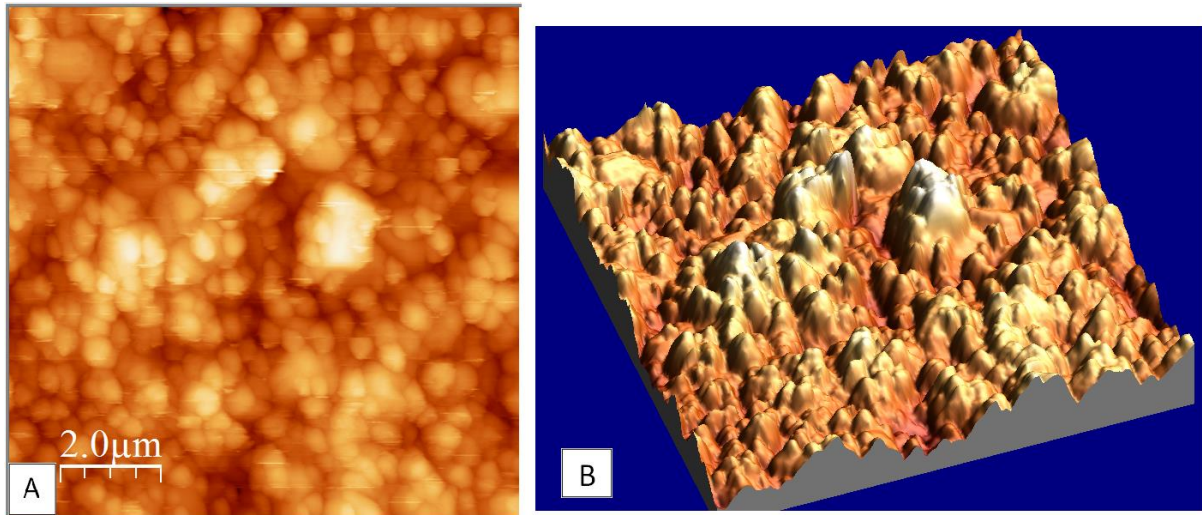


**Figure 23:** AFM images of the surface of substrate 1 taken after 4 hours UVO treatment. A) Shows a  $100 \mu\text{m}^2$  area of the sample B) Shows the same image as a three dimensional representation

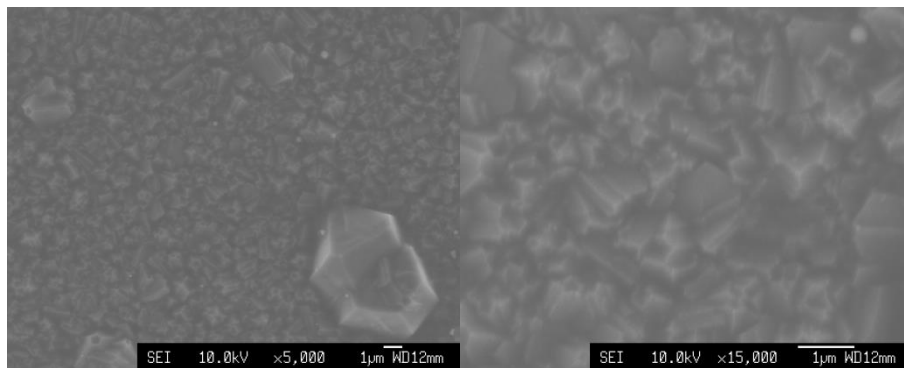


**Figure 24:** FEGSEM images of segment 1 of substrate 2 after UVO treatment. 2 hours of treatment were carried out on the surface. Images were taken at x5 000 and x15 000 magnification

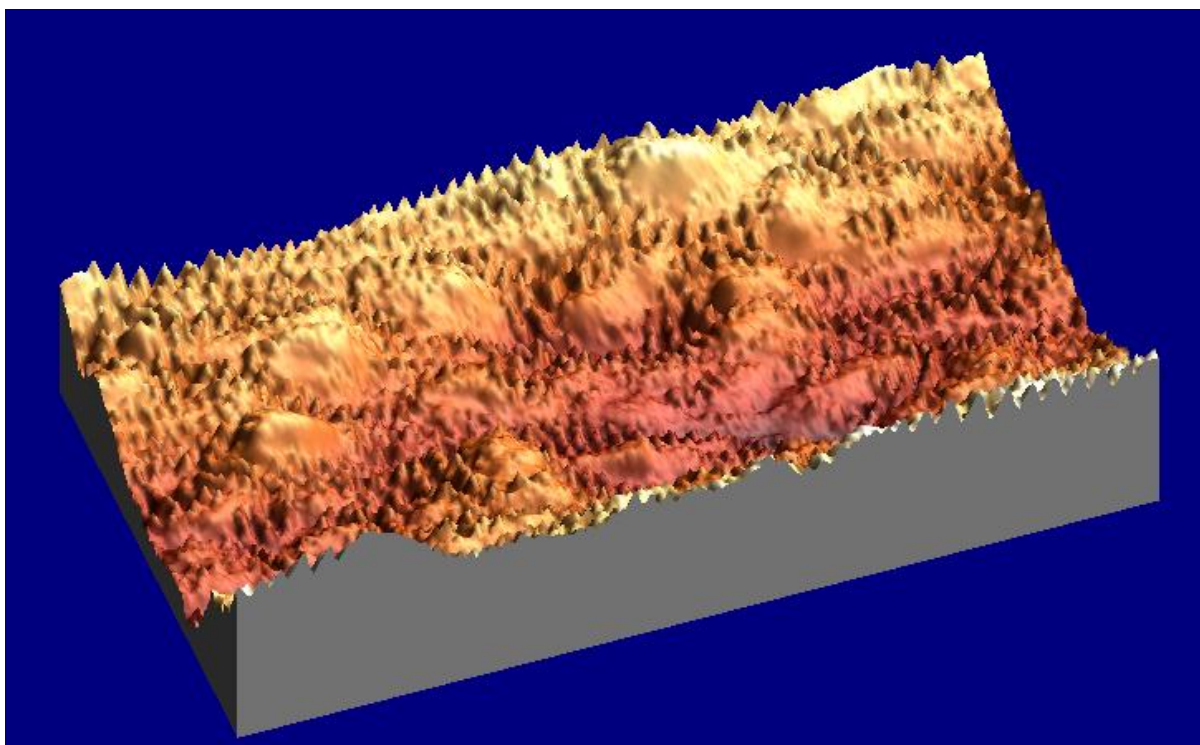


**Figure 25:** AFM image showing a three dimensional representation of the surface of segment 1 of substrate 2 after UVO treatment. 2 hours of treatment were carried out on the surface. The area shown is  $50 \mu\text{m}^2$

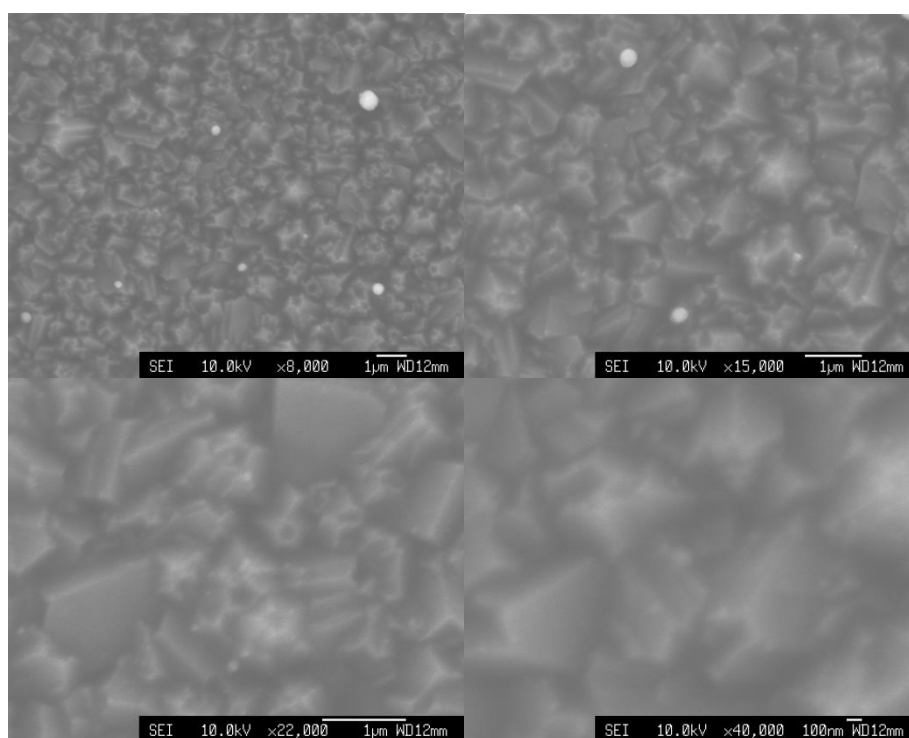


**Figure 26:** FEGSEM images of segment 2 of substrate 2 after UVO treatment. 4 hours of treatment were carried out on the surface. Images were taken at  $\times 8,000$ ,  $\times 15,000$ ,  $\times 22,000$  and  $\times 40,000$  magnification

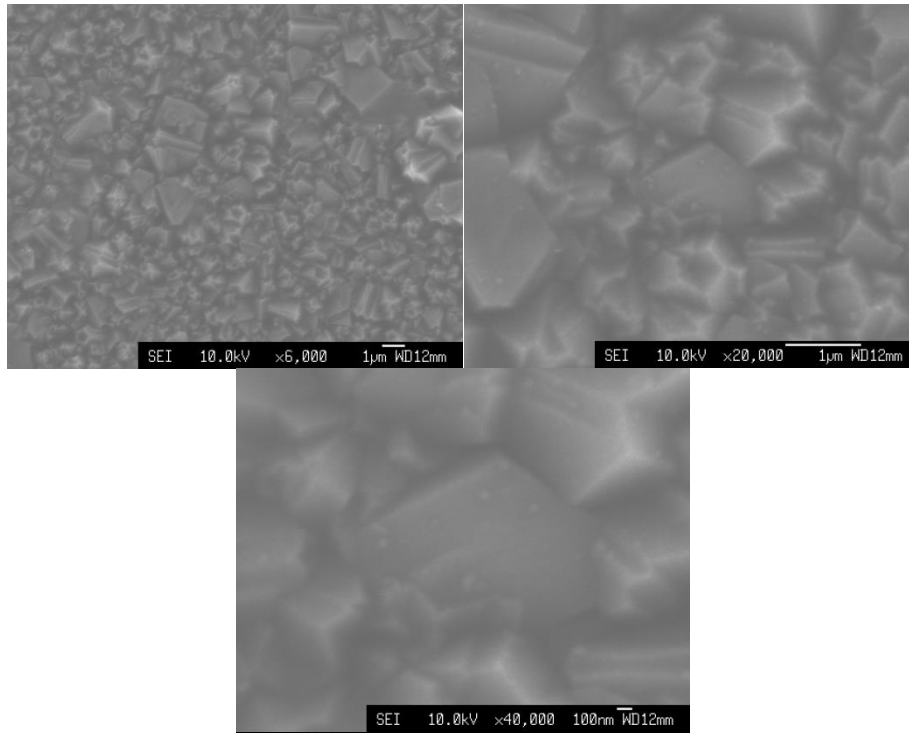


**Figure 27:** FEGSEM images of segment 3 of substrate 2 after UVO treatment. 6 hours of treatment were carried out on the surface. Images were taken at x6 000, x20 000 and x40 000 magnification

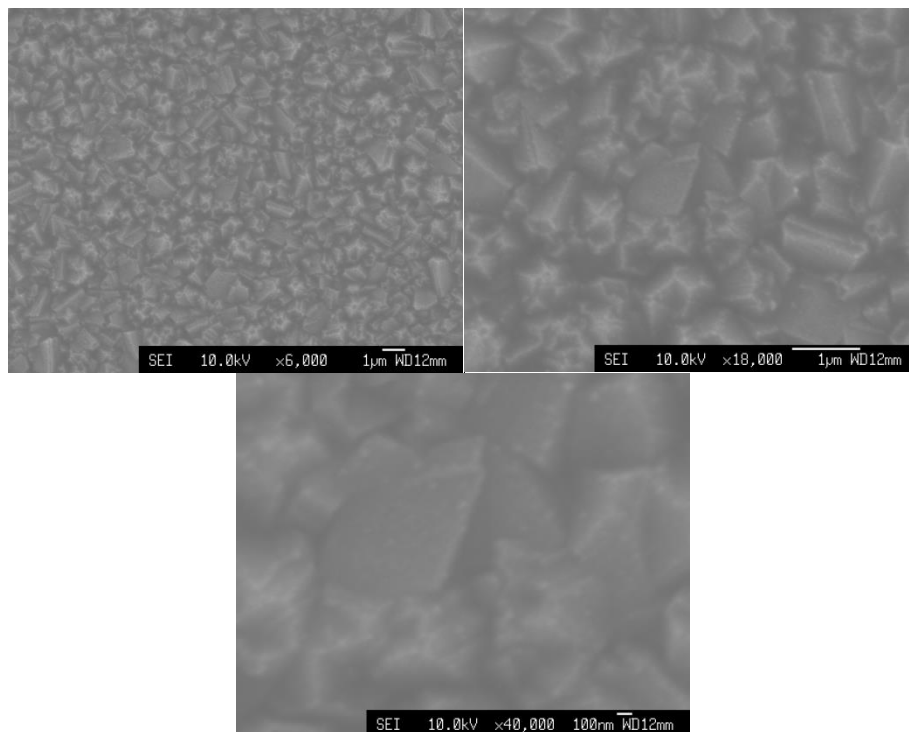


**Figure 28:** FEGSEM images of segment 4 of substrate 2 after UVO treatment. 8 hours of treatment were carried out on the surface. Images were taken at x6 000, x18 000 and x40 000 magnification

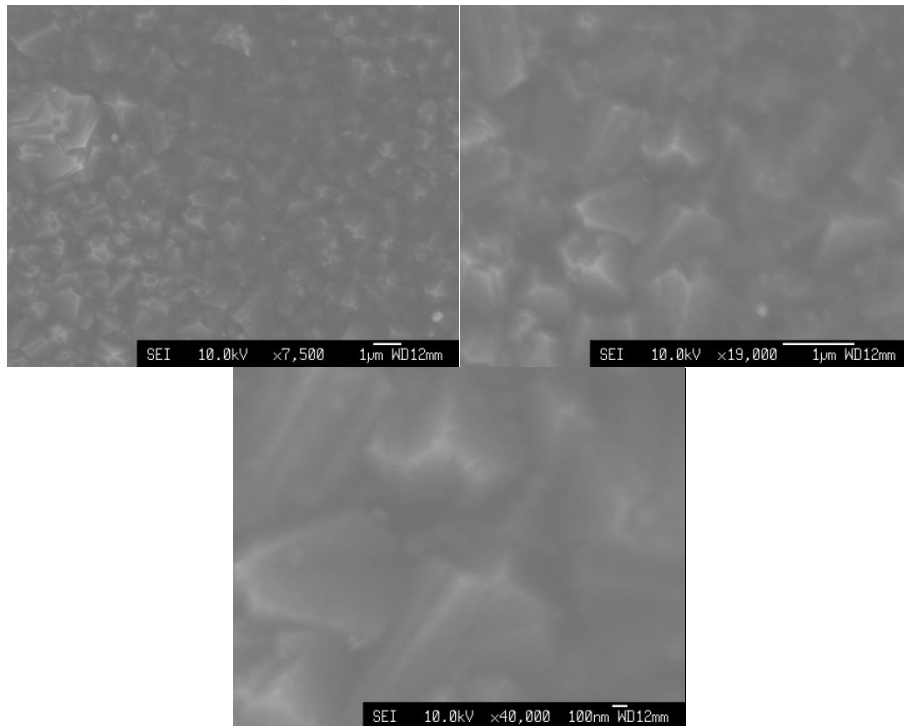


**Figure 29:** FEGSEM images of segment 5 of substrate 2 after UVO treatment. 10 hours of treatment were carried out on the surface. Images were taken at x7 500, x19 000 and x40 000 magnification

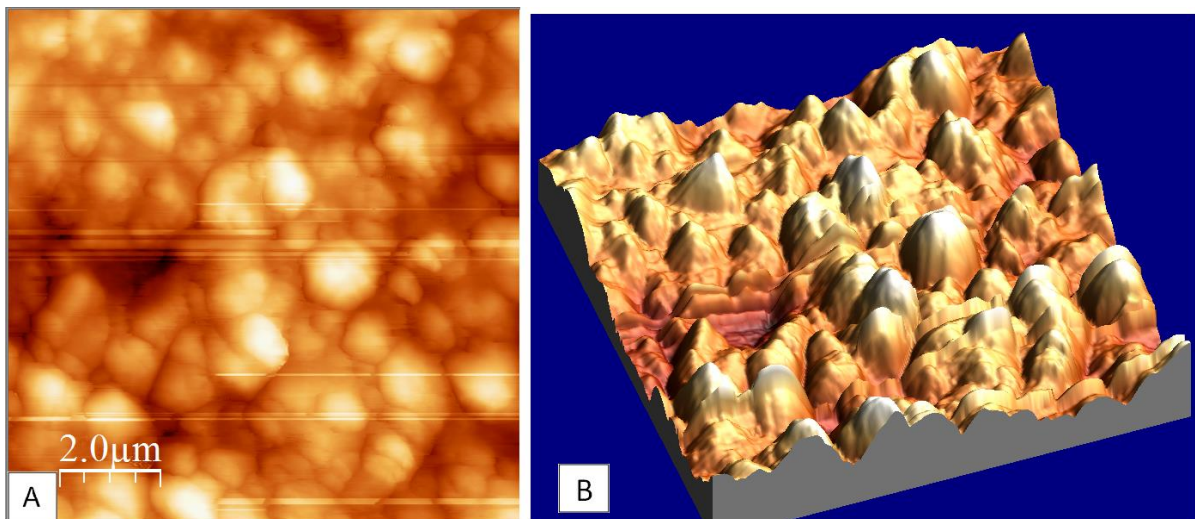


**Figure 30:** AFM images of the surface of segment 5 of substrate 2 taken after 10 hours UVO treatment. A) Shows a  $100 \mu\text{m}^2$  area of the sample B) Shows the same image as a three dimensional representation

### 3.3. Surface Roughness Analysis

An analysis of the effect that the UVO treatment had on the surface roughness of the substrates was carried out through the calculation of  $R_a$  and  $R_{RMS}$  values from the raw data of the surface topography obtained from the AFM, using equations 1 and 2.

Tables 1 – 4 give a summary of the surface roughness data gained from the AFM, and Figures 31 and 32 show a visual representation of the effect of different lengths of UVO treatment on the  $R_a$  and  $R_{RMS}$  character of the substrate surfaces.

Measurement	$R_a$ / nm	$R_{RMS}$ / nm
1	78.1	102.2
2	81.8	107.1
3	76.8	96.0
Average	78.9	101.8

**Table 1:** Surface roughness data of substrate 1 before UVO treatment

Hours Treatment	$R_a$ / nm	$R_{RMS}$ / nm
2	107.9	136.9
3	76.7	96.0
4	80.2	99.2

**Table 2:** Surface roughness data of substrate 1 after UVO treatment

Measurement	R <sub>a</sub> / nm	R <sub>RMS</sub> / nm
1	102.2	129.7
2	102.5	129.5
Average	102.4	129.8

**Table 3:** Surface roughness data of substrate 2 before UVO treatment

Segment	Hours Treatment	R <sub>a</sub> / nm	RRMS / nm
1	2	130.2	159.0
2	4	N/A	N/A
3	6	55.2	72.6
4	8	87.5	108.2
5	10	58.9	73.9

**Table 4:** Surface roughness data of the segments of substrate 2 after UVO treatment, data from segment 2 were unreadable

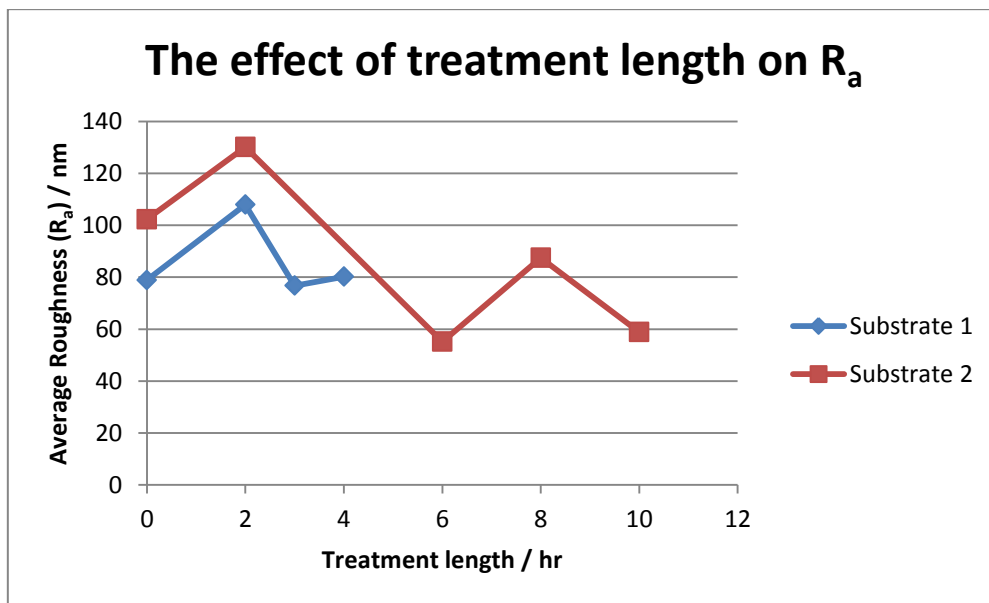


**Figure 31:** A graph showing a direct comparison between the average roughness of diamond surfaces and the length of UVO treatment received

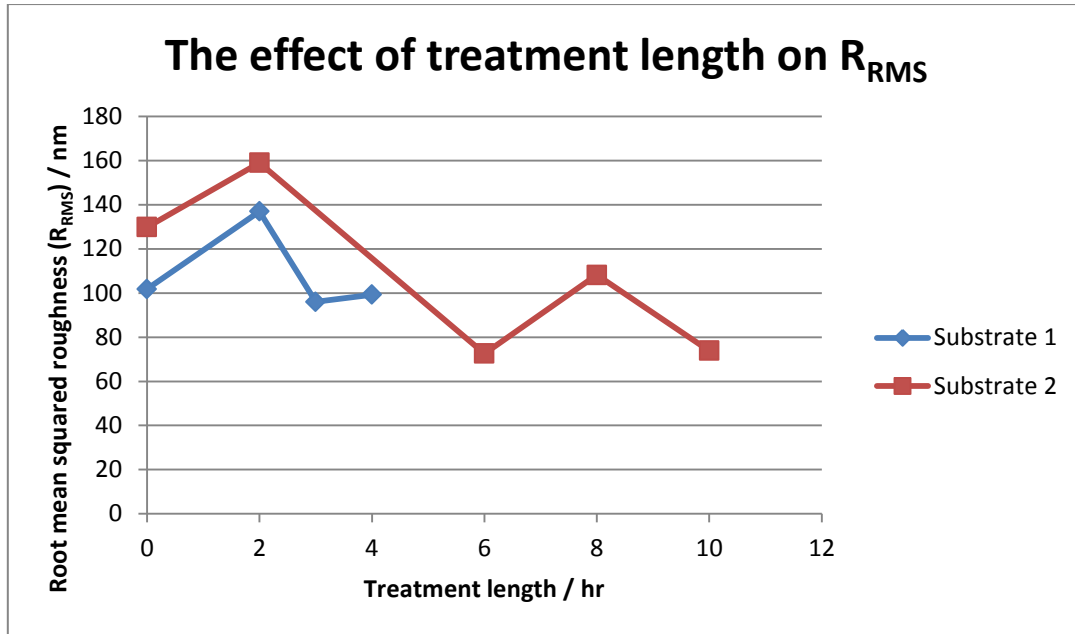


**Figure 32:** A graph showing a direct comparison between the root mean squared roughness of diamond surfaces and the length of UVO treatment received

# CHAPTER 4. DISCUSSION

## 4.1. Overview

The data gained from the imaging of the diamond surfaces before and after treatment can be used to gain insight into the use of UVO treatment as a viable process for non-contact polishing of diamond surfaces utilising dressed photon-phonon etching. There are a number of ways of looking at the data gained from the FEGSEM and AFM images; firstly, the images themselves can be examined in order to qualitatively analyse the visual effect that the UVO treatment appears to have had on the appearance and topography of the diamond surfaces. The numerical data concerning the roughness of the surfaces can then be utilised for quantitative analysis usage, so that direct comparisons can be made between the roughness values of the different surfaces after differing UVO treatment length times and thus the effect that UVO treatment had on the diamond surfaces can be ascertained.

## 4.2. Qualitative Analysis

The images gained from the FEGSEM and AFM show a number of interesting visual aspects of the diamond surfaces and the effect that the UVO treatment has had. Both the FEGSEM and AFM images of the pre-treatment surfaces clearly show that the samples being used are polycrystalline surfaces made up of diamond crystals of differing sizes, with the larger crystals roughly 1 micron and some smaller crystals being only a tenth of that size. This is shown in Figure 33 which re-iterates this point visually, showing the scale of the diamond surface. This microcrystal array clearly shows that the surface is very non-uniform, and the AFM pre-treatment images showing a representation of the topography of the surfaces affirm that they are far from being superflat surfaces.

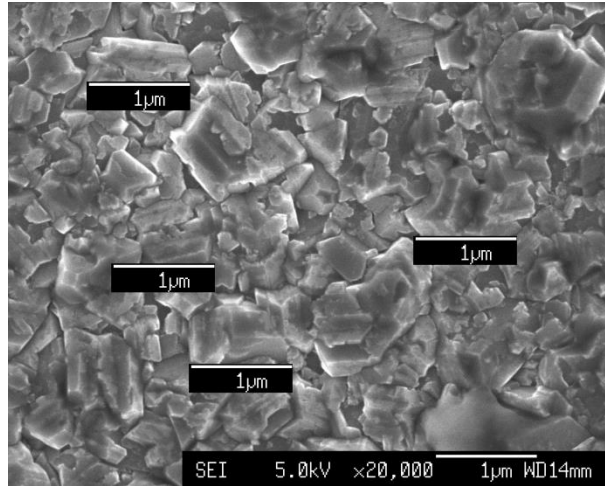


**Figure 33:** FEGSEM image of pre-treatment diamond surface showing the scale of the microcrystals. Image taken at x20 000 magnification

Although the microcrystals of the two substrate surfaces appeared to be on the same scale, the two substrates appeared to have a number of subtle visual differences. For example, substrate 2 appeared to have a number of imperfections on the surface of the microcrystals, whereas in substrate 1, the microcrystals appeared to have very few to no blemishes as shown in Figure 34. This could be due to a number of different reasons, such as the CVD diamond growth depositing a very small level of diamond on top of the existing microcrystals, giving the appearance of surface imperfections. However, this is an unlikely scenario and what is the most likely case is that these blemishes are simply small dust particles that have become deposited on the surface. This could be due to an unclean storage area with dust particles present even though an attempt was made at all times to keep the storage environment clean, or also unclean apparatus used to insert the substrate into the FEGSEM and transport the substrate in and out of the storage area.

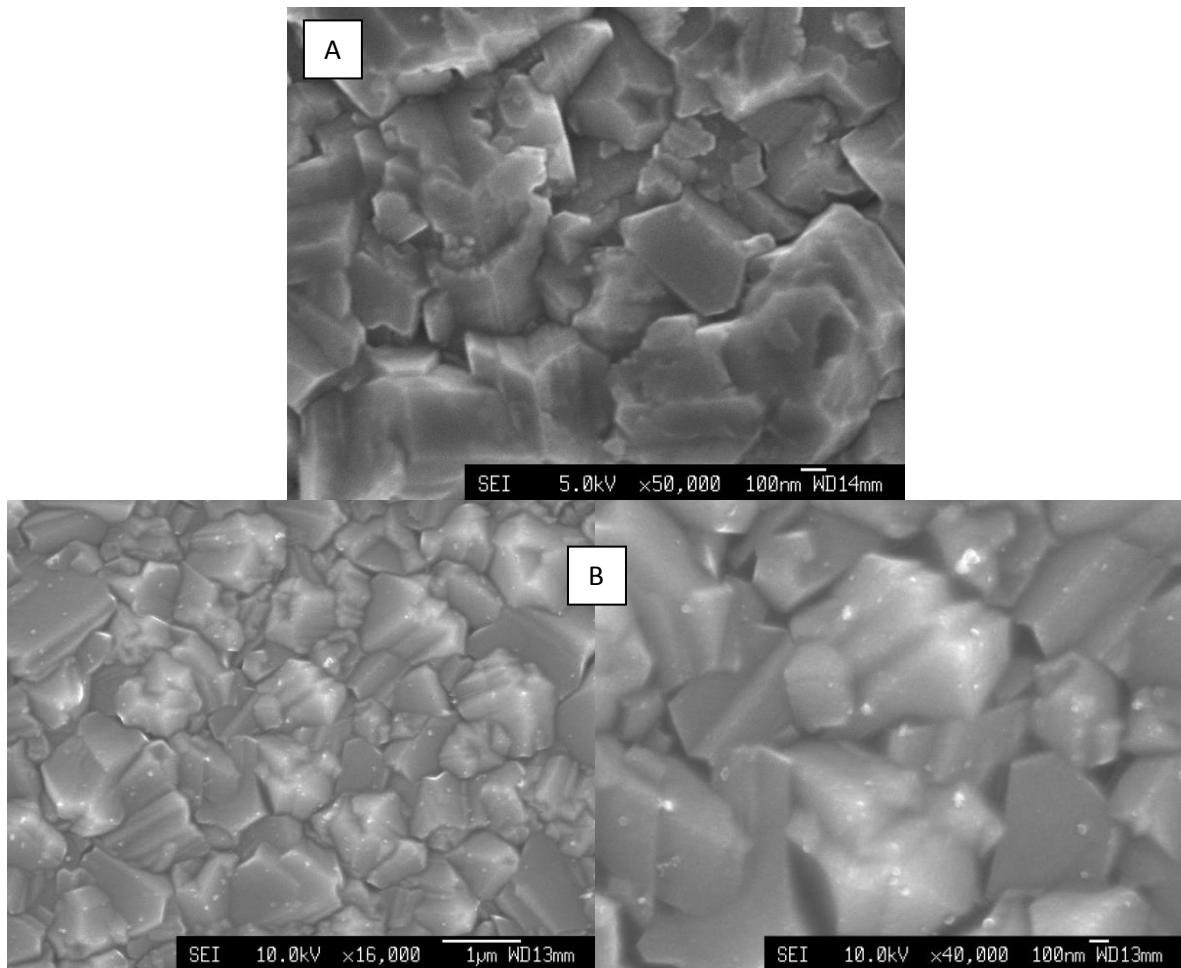


**Figure 34:** A side by side comparison of the surfaces of substrates 1 and 2. A) The surface of substrate 1 taken at x50 000 magnification showing the minimal number of imperfection on the microcrystal surface. B) The surface of substrate 2 showing a number of blemishes on the microcrystals. Shown at x16 000 and x40 000 magnification to demonstrate that the blemishes are not a localised problem

After a level of UVO treatment was applied to the substrates, a number of visual differences became apparent on the diamond surfaces. On substrate 1, the diamond surface appeared to gain a large number of imperfections after only 1 hour treatment as shown in Figure 36. From the FEGSEM images it is very difficult to discern whether these imperfections are protruding from the surface or depressions in the surface. If the imperfections are depressions into the surface, this is a good indication that the treatment is having an effect on the topography of the surface by etching into the surface and thus would be proof that dressed photon-phonon etching is occurring. However, it is not possible to tell from the FEGSEM images taken that this phenomenon is occurring. The imperfections gained after UVO treatment have a very different appearance to the imperfections on substrate 2 before

any UVO treatment takes place, appearing to be much larger and more crystalline. This is why it is not thought that the imperfections on substrate 1 are also dust particles.

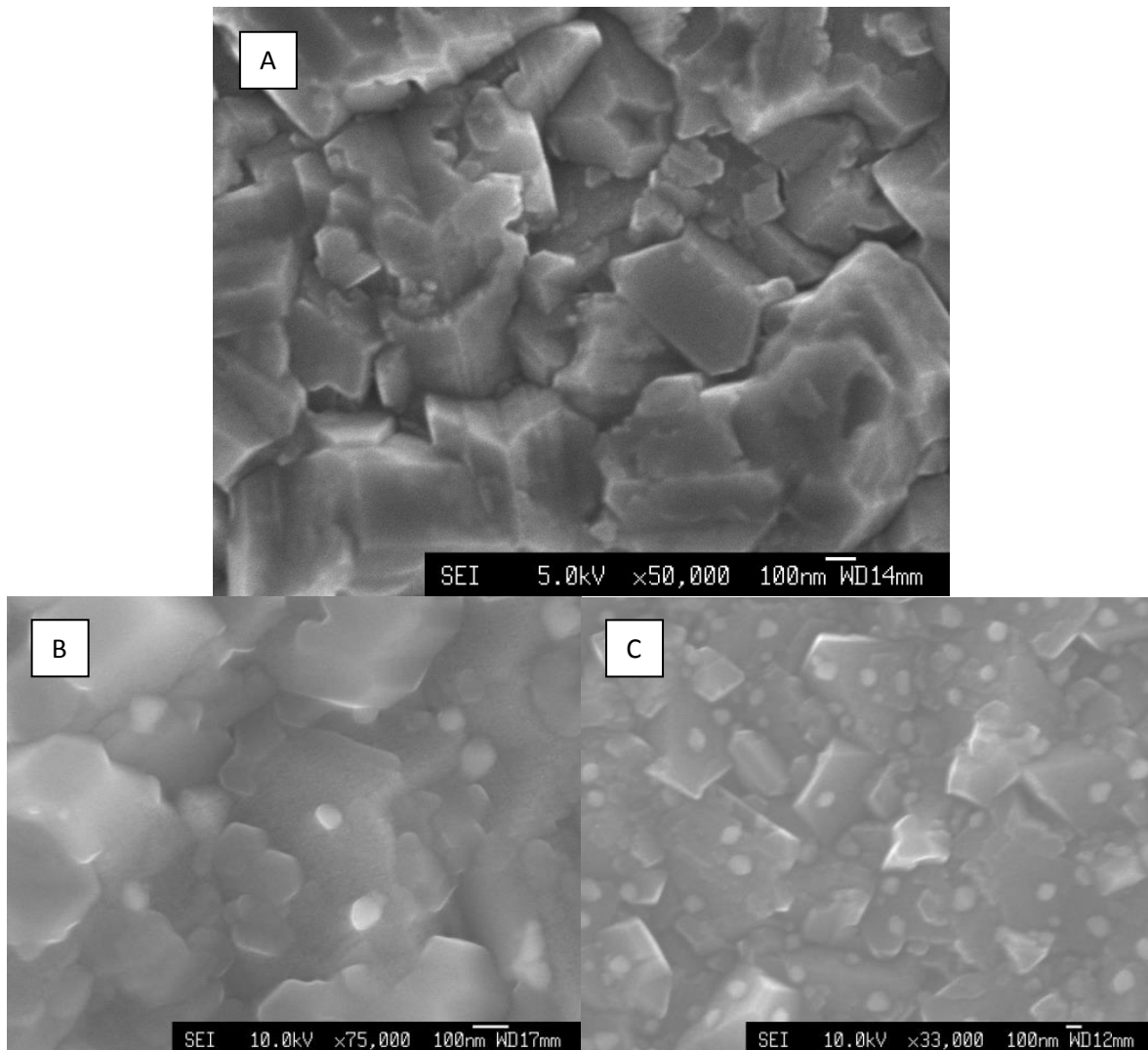


**Figure 36:** FEGSEM images showing the effect of UVO treatment on surface imperfections on substrate 1. A) Pre-treatment image at x50 000 magnification. B) After 1 hour UVO treatment at x75 000 magnification. C) After 2 hours UVO treatment at x33 000 magnification

The FEGSEM images of substrate 2 also show that the UVO treatment has had an effect on the visual appearance of the diamond surface. It appears that the peaks on the surface have become more rounded after treatment as shown in the comparison between pre-treatment and post-treatment FEGSEM images in Figure 37. But this is clearly an unquantifiable property from the FEGSEM images and determining surface topography through visual images is an inexact science by definition so this is not hard evidence of dressed photon-

phonon etching occurring. However, the imperfections that were thought to be dust particles seem to be gone after UVO treatment has been performed on the substrate. This is not a surprising result seeing as the main use of the UVO Cleaner is to clean hydrocarbon residuals and other impurities off surfaces. Thus it can be expected that a certain level of cleaning could have occurred even with the presence of the diamond window.

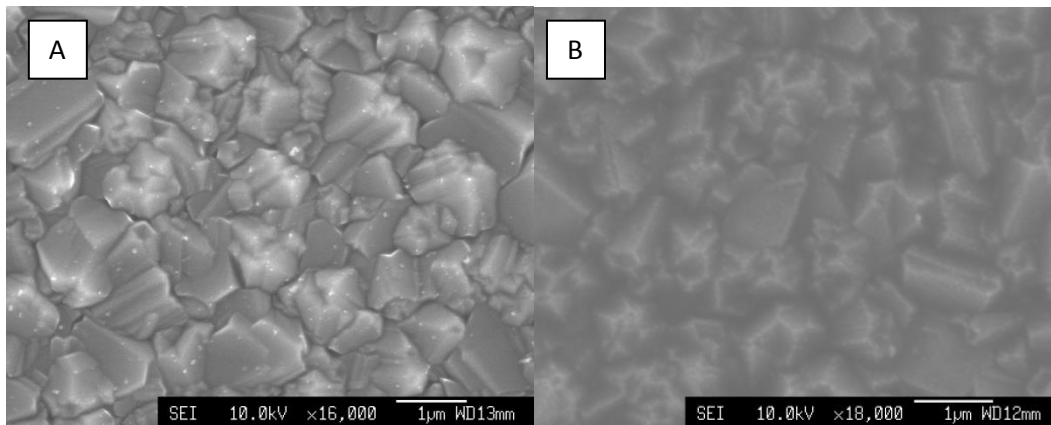


**Figure 37:** FEGSEM images showing visual effects of UVO treatment on substrate 2. A) Pre-treatment image at x16 000 magnification. B) Image of surface after 6 hours UVO treatment at x18 000 magnification

The AFM images gave a three-dimensional representation of the diamond surfaces which are very useful in showing the visual changes to the topography of the diamond surfaces. Figure 38 shows that the peaks seem to be more rounded after 4 hours of UVO treatment. However the effect that the treatment has had on the surface does not seem to be very great and the visual difference between the pre-treatment and post-treatment images is quite minimal. This gives the indication that the UVO treatment has not had a great effect on the diamond surface.

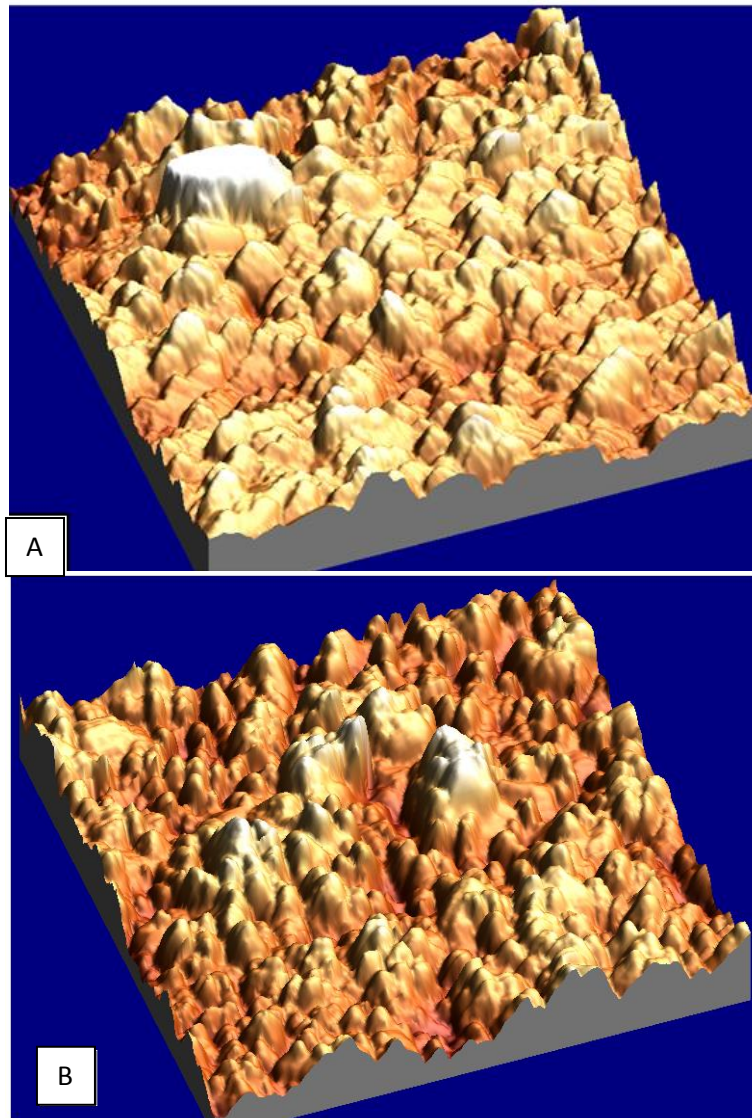


**Figure 38:** AFM images showing comparison of the surface of substrate 1 before and after UVO treatment. A) Pre-treatment AFM image of  $100\ \mu\text{m}^2$  area of substrate 1. B) AFM image of  $100\ \mu\text{m}^2$  area of substrate 1 after 4 hours UVO treatment

AFM images of substrate 2 seem to show that the UVO treatment has had an effect on the topography of the surface. After 10 hours of treatment the peaks of the surface appear to be a lot smoother and more rounded than the images pre-treatment as shown in Figure 39. This indicates that the signs that substrate 1 was showing of rounded peaks would become more greatly exaggerated after more hours of UVO treatment, and the levels of treatment given were not high enough for any large discernible effect to be observed. The 10 hours treatment given to substrate 2 gives a much more visual effect and this gives good evidence that the UVO treatment is having an effect on the topography of the diamond surface, but

without analysing the quantitative data, the extent to which the surface roughness is changing cannot be determined.

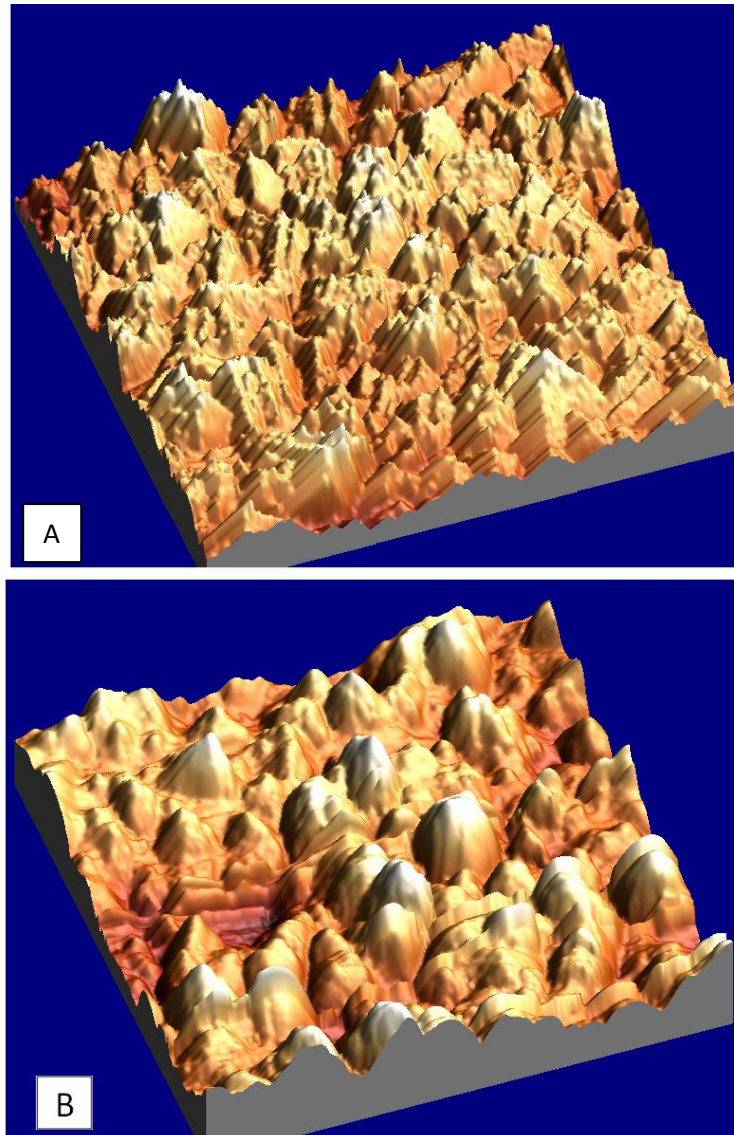


**Figure 39:** AFM images demonstrating the effect UVO treatment has had on the topography of the surface of substrate 2. A) Pre-treatment AFM image of  $100 \mu\text{m}^2$  area of substrate 2. B) AFM image of  $100 \mu\text{m}^2$  area of substrate 2 after 10 hours UVO treatment

### 4.3. Quantitative Analysis

The data from the AFM images show the surface roughness of the substrates. This can then be analysed to compare the effect of different lengths of UVO treatment on the diamond surfaces. Figures 31 and 32 show the effect of different lengths of treatment on the surface roughness of the diamond substrates. Figures 40 and 41 show a readjustment of the data, showing a direct comparison of the  $R_a$  and  $R_{RMS}$  for each substrate. The relationship between  $R_a$  and  $R_{RMS}$  is clearly shown in the two figures, the  $R_a$  is very similar to  $R_{RMS}$  and follows the same trend but the values are slightly higher. This is because  $R_a$  is unable to account for the differences between peaks and troughs in an area of the surface, as has previously been mentioned.

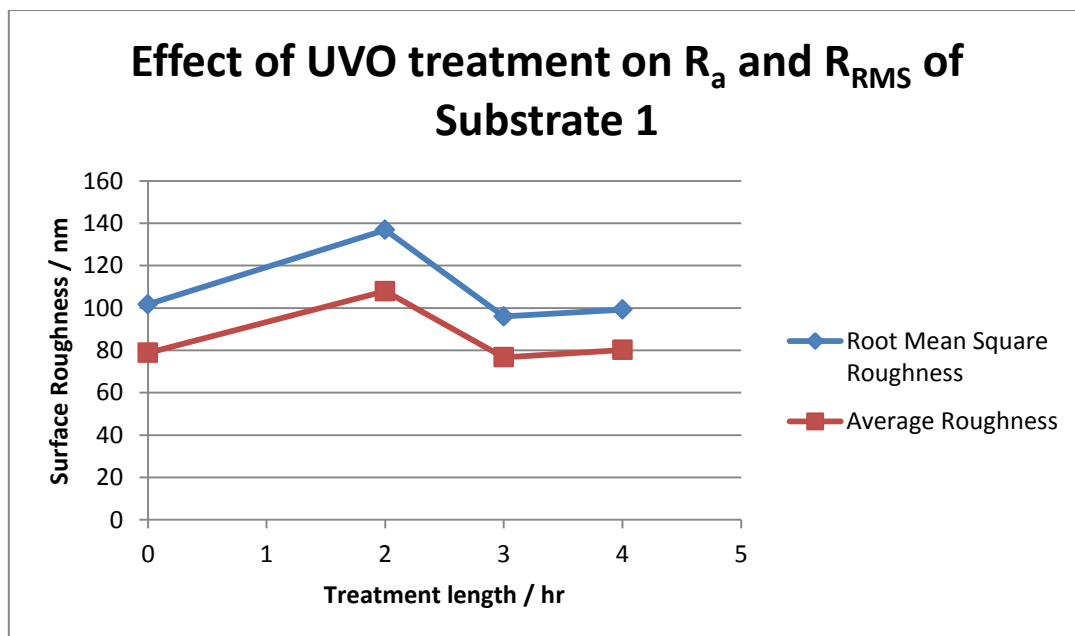


**Figure 40:** Graph showing the effect of UVO treatment on the average roughness and root mean square roughness of the surface of substrate 1

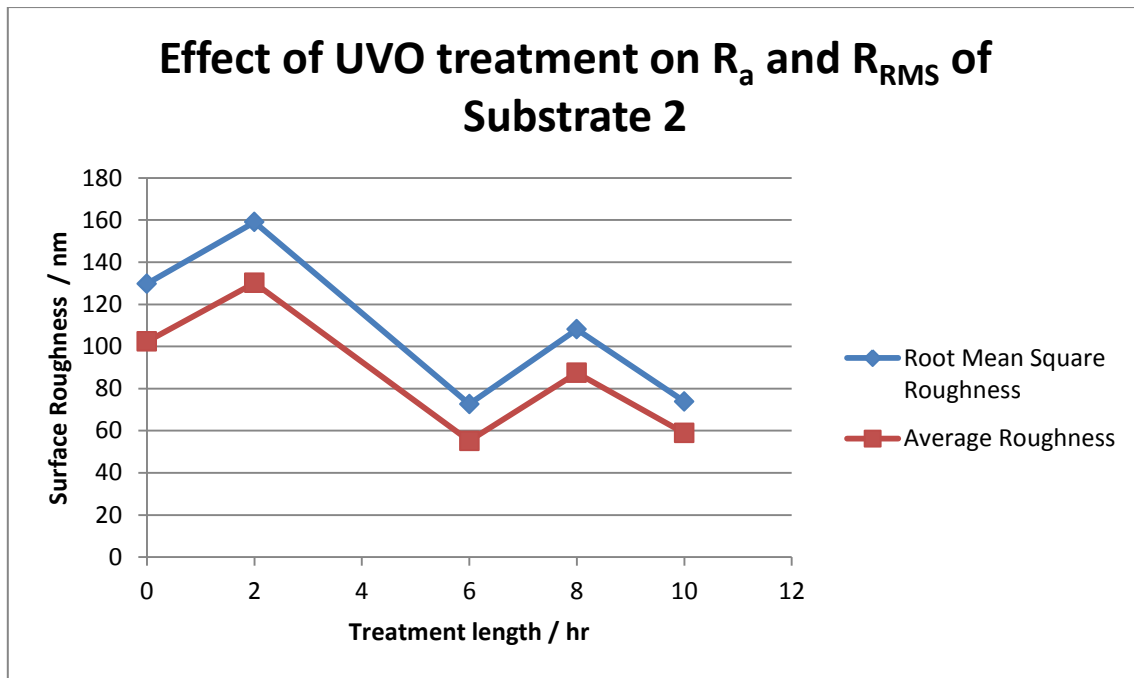


**Figure 41:** Graph showing effect of UVO treatment on average roughness and root mean square roughness of the surface of substrate 2

The effect of the UVO treatment on the surfaces can be analysed using the data shown in Figures 40 and 41. The analysis of the surface roughness of substrate 1 seems to show that there is no numerical evidence that the UVO treatment has decreased the roughness of the surface. Figure 40 shows that the average roughness and root mean squared roughness of the surface of substrate 1 seems to have increased after UVO treatment which is very counter-intuitive. However, there is a quintessential issue with the surface roughness measurements which is that they only measure the roughness of a  $100 \mu\text{m}^2$  area. This is a very small proportion of the  $1 \text{ cm}^2$  substrate, 6 orders of magnitude smaller, and thus even if the surface roughness has been reduced by the treatment, it is extremely unlikely that the same area of the surface will be measured, and due to the non-uniform character of the surface, the surface topography can vary drastically in different areas of the surface, and thus the UVO treatment can appear to have increased the surface roughness when this is not the case. A simple solution to this problem would be to have large numbers of measurements at each point and take an average of the measurements. However this solution was impractical for this project because each AFM image takes over an hour to capture and the time constraints on the project made this an unfeasible solution, but if the time constraint was taken away; this would be a possible solution to finding evidence that substrate 1 was affected or unaffected by the UVO treatment instead of the inconclusive trend that is shown in Figure 40.

The UVO treatment had a much clearer effect on substrate 2 than the effect observed on substrate 1. There is a clear trend in Figure 41 showing that both the average roughness and the root mean square average roughness decrease as the length of the UVO treatment increases which is a good indication that UVO treatment decreases the surface roughness of diamond surfaces. However, as discussed above, these results may not be completely reliable due to the lack of ability to perform a large number of measurements and thus the data are based on only one measurement for each segment and not an average of many measurements. Although this may be an issue showing the unreliability of the substrate 2 measurements, the substrate 2 data are more reliable than the substrate 1 data, due to the fact that the measurements were taken almost simultaneously due to the substrate being split into segments with each segment receiving a different level of UVO treatment, thus substrate 2 is in 5 states of treatment length simultaneously. This means that the condition of the segments was very similar, whereas with substrate 1 the measurements were taken at various times throughout the project and the condition of the substrate may have changed over that time due to external stimuli.

The results obtained through this project do not compare well to the results attained by Yatsui *et al.* who gained clear evidence of dressed photon-phonon etching on a single crystalline diamond surface after only 30 minutes, with  $R_a$  reducing from 0.660 nm to 0.242 nm<sup>1</sup>. However, the roughness of the single crystalline surface before any treatment took place is miniscule compared to the surface roughness of the multicrystalline diamond surfaces used in this project. Yatsui *et al.* started with  $R_a$  of 0.660 nm whereas the diamond surfaces used in this project started with  $R_a$  of 80 – 100 nm, 2 orders of magnitude larger. Thus, for an effect on the surface roughness to be seen after only 10 hours of UVO treatment is promising, although investigations into whether this trend continues after large increases in the length of UVO treatment must be conducted in further work.

All in all, the data collected from the AFM images seem to show inconclusive data for substrate 1 but also seem to quantify that substrate 2 has gone through a level of non-contact polishing by dressed photon-phonon etching, over a period of 10 hours. Although the etching is not on the same scale as the non-contact polishing attained by Yatsui *et al.* and the data may not be completely reliable due to the low number of measurements obtained, the result appears to be positive.

# CHAPTER 5. CONCLUSION

## 5.1. Overview

The quantitative data collected seemed to show that the surface roughness of substrate 2 decreased to some degree after UVO treatment due to dressed photon-phonon etching. Substrate 1 may have showed similar trends if more hours of treatment were undertaken and this is a recommended course of action for future experimentation.

The qualitative and quantitative data seem to corroborate in suggesting that the surface roughness of substrate 2 was decreased throughout the project due to the surface peaks appearing more rounded after UVO treatment than the original surface peaks and the  $R_a$  and  $R_{RMS}$  values showing a downward trend as UVO treatment length increases.

However, the data gathered show that the results obtained for the multicrystalline surfaces are not comparable to the results attained by Yatsui *et al.* with a single crystal diamond surface, and thus suggests that realisation of superflat surfaces through dressed photon-phonon is much more challenging on multicrystalline surfaces than on a single crystal diamond surfaces.

In conclusion, although signs of the surface roughness decreasing are present, the evidence gathered by this project is not extensive enough to prove that dressed photon-phonon etching successfully occurred, so it cannot be concluded that non-contact polishing of multicrystalline diamond surfaces was successfully observed. The evidence suggests that this is the case but further experimentation is needed to obtain proof to confirm these findings.

For future work, a recommended course of action would be to greatly increase the number of hours of UVO treatment undertaken in order to discover whether the trends seen in the data continue. Also, the number of AFM measurements taken at each stage should be hugely increased in order to calculate an average of the surface roughness so that more reliable data can be gathered. Another approach is to synthesise a number of diamond substrate with varying levels of doping in order to investigate whether this assists or hinders dressed photon-phonon etching.

Once evidence has been found to confirm or refute the conclusions gained from this project, further steps into the research can be taken. If proof of dressed photon-phonon is found, the next step would be to investigate whether the dressed photon-phonon etching affects the termination of the diamond surface by metals, and what the effect of the etching is on the contact potential difference of the diamond surface, with the aim of producing a highly uniform contact potential difference across a superflat surface for potential use in high performance applications.

# References

- 
- <sup>1</sup> Yatsui, T., Nomura, W., Naruse, M., Ohtsu, M., *J. Phys. D: Appl. Phys.*, **45**, 475302, (2012).
  - <sup>2</sup> Pierson, H. O., *Handbook of Carbon, Graphite, Diamond and Fullerene: Properties, Processing and Applications*, (1993).
  - <sup>3</sup> Wilks, J., Wilks, E., *Properties and applications of diamond*, 525, Oxford: Butterworth-Heinemann (1991).
  - <sup>4</sup> Chong, H. H., *et al.*, *Mater. Sci. Forum.*, **505 - 507**, 1225 - 1230, (2006).
  - <sup>5</sup> Spear, K. E., Dismukes, J. P., eds. *Synthetic Diamond: Emerging CVD Science and Technology*, Vol. 25, 4, John Wiley & Sons, (1994).
  - <sup>6</sup> G. Heinrich, T. Grögler, S.M. Rosiwal, R.F. Singer, CVD diamond coated titanium alloys for biomedical and aerospace applications, *Surface and Coatings Technology*, **94 – 95**, 514-520, (1997).
  - <sup>7</sup> W. Ebert, M. Adamschik, P. Gluche, A. Flöter, E. Kohn, High-temperature diamond capacitor, *Diamond Relat. Mater.*, **8**, 10, 1875-1877, (1999).
  - <sup>8</sup> Kania, D. R., *et al.* "Diamond radiation detectors." *Diamond Relat. Mater.* **2.5**, 1012-1019 (1993).
  - <sup>9</sup> Paradis, L. R., *et al.* "Diamond heat sink." U.S. Patent No. 20,030,183,368. (2003).
  - <sup>10</sup> Sussmann, R. S., *et al.* "CVD diamond: a new engineering material for thermal, dielectric and optical applications." *Industrial Diamond Rev.*, **58.578**, 69 - 77, (1998).
  - <sup>11</sup> Bundy, F. P., Hall, H. T., Strong, H. M. & Wentorf, R. H. Jr *Nature* **176**, 51-54 (1955).
  - <sup>12</sup> Bundy, F.P. *et al.* Jr *Nature* **365**, 19 (1993).
  - <sup>13</sup> Bovenkerk, H. P., Bundy, F. P., Hall, H. T., Strong, H. M. & Wentorf, R. H. Jr *Nature* **184**, 1094-1098 (1959).
  - <sup>14</sup> Eversole, W. G., U.S. Patent Nos. 3030187 and 303 018 (1958).
  - <sup>15</sup> Deryagin, B. V., Fedoseev, D. V., Lukyanovich V. M., Spitsyn, B. V., Ryanov, A. V., Lavrentyev, A. V., *J. Cryst. Growth*, **2**, 380 (1968).
  - <sup>16</sup> Angus, J. C., Will, H. C., Stanko, W. S., *J. Appl. Phys.* **39**, 2915 (1968).
  - <sup>17</sup> Deryagin, B. V., Fedoseev, D. V., *Russ. Chem. Rev.*, **39**, 783, (1970).
  - <sup>18</sup> Balmer, R. S., *et al.*, *J. Phys.*, **21**, 36, 364221, (2009).
  - <sup>19</sup> Spitsyn, B. V., Bouilov, L. L., Derjaguin, B. V, *J. Cryst. Growth*, **52**, 219-226, (1981).
  - <sup>20</sup> Frenklach, M., *J. Appl. Phys.*, **65**, 5142, (1989).
  - <sup>21</sup> Harris, S. J., *Appl. Phys. Lett.*, **56**, 2298, (1990).
  - <sup>22</sup> Ashfold, M. N. R. A., May, P. W., Rego, C. A., Everitt, N. M., *Chem. Soc. Rev.*, **1**, 21-30 (1994).
  - <sup>23</sup> Singh, J., "Nucleation and growth mechanism of diamond during hot-filament chemical vapour deposition", *J. Mat. Sci.*, **29**, 2761 – 2766 (1994).
  - <sup>24</sup> Angus, J. C., Hayman, C. C., *Science*, **241**, 4868, 913-921 (1988).
  - <sup>25</sup> Ralchenko, V. G. *et al.*, *Diamond Relat. Mater.*, **6**, 417, (1997).
  - <sup>26</sup> Suzuki, K. *et al.*, "Growth of diamond thin films by dc plasma chemical vapour deposition", *Appl. Phys. Lett.*, **50**, 728 (1987).
  - <sup>27</sup> Denisenko, A., Kohn, E., "Diamond power devices. Concepts and limits", *Diamond Relat. Mater*, **14**, 3-7 (2005).
  - <sup>28</sup> Makino, T., Tokuda, N. *et al.*, "Electrical and light-emitting properties of homoepitaxial diamond p–i–n junction", *Phys. Status Solidi A*, **205**, 2200–2206 (2008).
  - <sup>29</sup> Malshe, A. P., Park, B. S., Brown, W. D., Naseem, H. A., *Diamond Relat. Mater.*, **8**, 1198-1213, (1999).
  - <sup>30</sup> Myers, N. O., "Characterization of surface roughness", *Wear*, **5**, 182-189 (1962).
  - <sup>31</sup> Tak, Y. H., Kim, K. B., Park, H. G., Lee, K. H., Lee, J. R., "Criteria for ITO (indium–tin-oxide) thin film as the bottom electrode of an organic light emitting diode", *Thin Solid Films*, **411**, 1, 12-16 (2002).
  - <sup>32</sup> Marnett, L. J., Reddy, A., Pruess-Schwartz, D., Ji, C., *Princess Takamatsu Symp.*, **21**, 63-73, (1990).
  - <sup>33</sup> Kappes, M. M., Staley, R. H., *J. Phys. Chem.*, **85**, 942-944, (1981).
  - <sup>34</sup> Ohtsu, M., "Dressed photon technology", *Nanophotonics*, **1**, 83-97 (2012).
  - <sup>35</sup> Kobayashi, K., Sangu, S., Ito, H., Ohtsu, M., "Near-field optical potential for a neutral atom", *Phys. Rev. A*, **63**, 013806, (2001).
  - <sup>36</sup> Tanaka, Y., Kobayashi, K., *J. Microsc.*, **229**, 228-232, (2008).
  - <sup>37</sup> Sato, A., "Photon localization and tunnelling in a disordered nanostructure), *J. Luminesc.*, **129**, 1718-1721, (2009).
  - <sup>38</sup> Kobayashi, K., Kawazoe, T., Ohtsu, M., *Trans. Nanotech.*, **4**, 517-522, (2005).